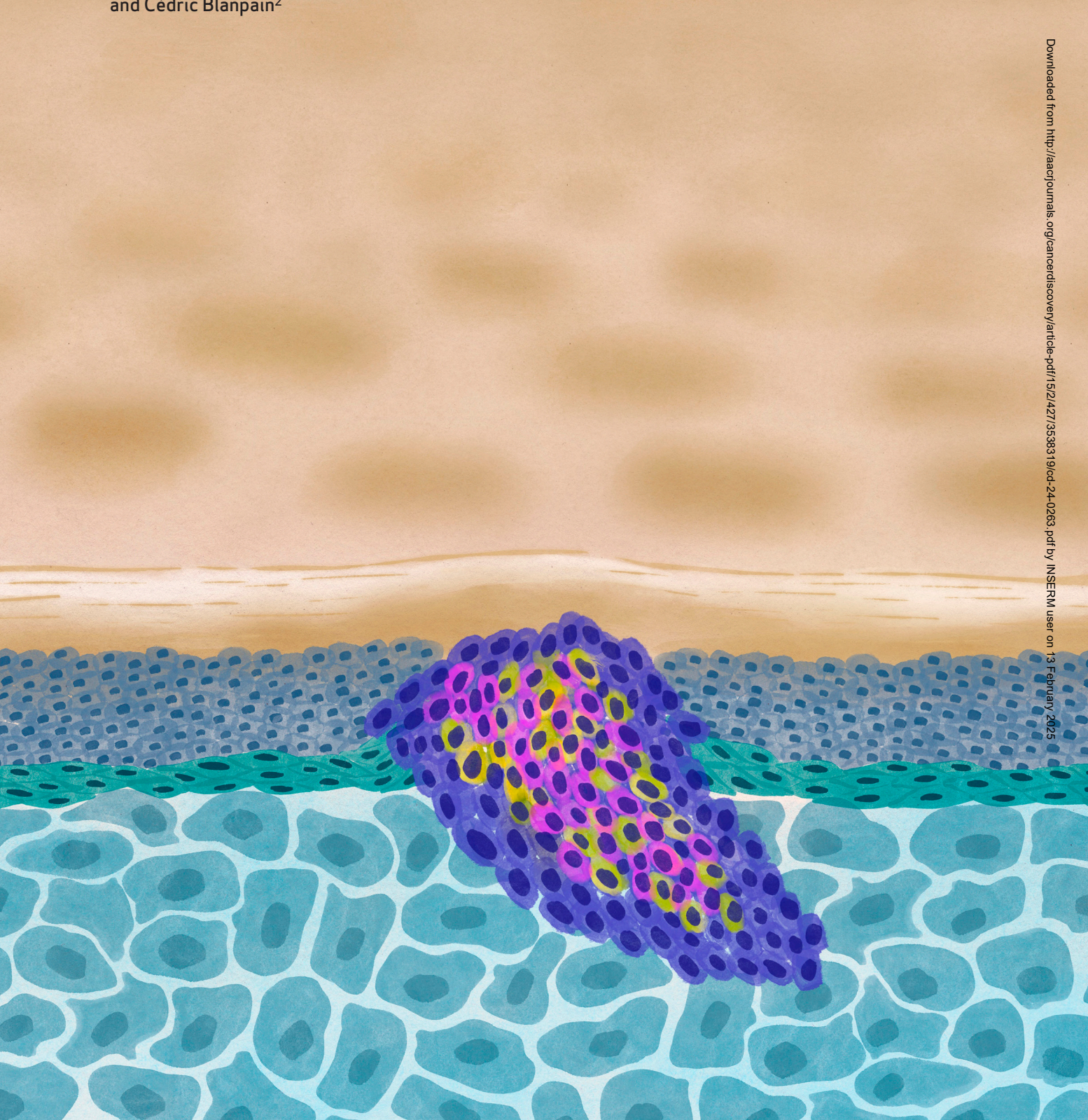
Survivin Promotes Stem Cell Competence for Skin Cancer Initiation

Sara Canato¹, Rahul Sarate², Sofia Carvalho-Marques¹, Raquel Maia Soares¹, Yura Song², Sara Monteiro-Ferreira¹, Pauline Vieugué², Mélanie Liagre², Giancarlo Grossi³, Erik Cardoso¹, Christine Dubois², Edward M. Conway⁴, Silvia Schenone³, Adriana Sánchez-Danés¹, and Cédric Blanpain²



ABSTRACT

Stem cells (SC) and not progenitors (P) act as cells of origin of basal cell carcinoma (BCC). The mechanisms promoting BCC formation in SCs or restricting tumor

development in Ps are currently unknown. In this study, we transcriptionally profiled SCs and Ps and found that *Survivin*, a pleiotropic factor that promotes cell division and inhibits apoptosis, was preferentially expressed in SCs. Using genetic gain- and loss-of-function mouse models, we showed that *Survivin* deletion in oncogene-expressing SCs prevents BCC formation. *Survivin* overexpression renders Ps competent to BCC formation by promoting cell survival and division while preventing apoptosis and differentiation. We identified *Serum glucocorticoid-regulated kinase* 1 (*Sgk1*) as a key downstream factor of *Survivin* and that its inhibition prevents BCC formation. This study uncovers the role and mechanisms by which *Survivin* regulates the competence of SCs to initiate BCC formation, promoting the survival of oncogene-expressing SCs and self-renewing division while restricting differentiation and apoptosis.

SIGNIFICANCE: This study identifies *Survivin* as a key regulator of the different ability of SCs and Ps to initiate skin cancer. *Survivin* expression in oncogene-targeted SCs is essential for their survival and self-renewal and to prevent their differentiation and apoptosis, allowing SCs and not Ps to initiate skin cancer.

INTRODUCTION

Homeostasis of the skin interfollicular epidermis (IFE) is maintained by heterogeneous populations of stem cells (SC) and progenitors (P) located in the basal compartment. Lineage-tracing studies have shown that *Krt14-CREER* mice target SCs and Ps, whereas *Inv-CREER* mice preferentially target Ps (1–3).

Basal cell carcinoma (BCC) is the most frequent cancer in humans (4). BCC arises upon constitutive activation of the Hedgehog (Hh) signaling pathway through either *Patched 1* (*Ptch1*) loss-of-function or *Smoothened* (*Smo*) gain-of-function mutations (4). In mice, BCC arises preferentially from SCs located in the IFE and infundibulum (5–7). Within the IFE, SCs and Ps present different competence to induce BCC formation. Activation of the Hh signaling pathway through deletion or activation of the active form of *Smoothened* (*SmoM2*) in SCs using the *Krt14-CREER* lead to BCC formation (2). By contrast, oncogenic activation of the Hh pathway with the same oncogenic hit in Ps using *Inv-CREER* lead to the formation of

lesions that were frozen in their preneoplastic stage and did not progress into invasive BCC (2). The mechanisms that confer competence to BCC formation in the epidermal SCs and restrict BCC development in Ps remain unresolved.

In this study, we have assessed the mechanisms that confer competence of SCs to BCC initiation in mice. Using transcriptional profiling, we have uncovered that baculoviral inhibitor of apoptosis repeat–containing protein 5 (Birc5)/Survivin is preferentially expressed in oncogene-expressing SCs compared with oncogene-expressing Ps. By using the gain and loss of functions of Survivin in vivo, we showed that Survivin expression is required for BCC initiation by promoting cell survival and proliferation, as well as in restricting terminal differentiation of oncogene-expressing cells. Finally, we showed that Survivin mediates BCC initiation through upregulation of serum glucocorticoid–regulated kinase 1 (Sgk1), uncovering a new pharmacologic approach to prevent BCC formation.

¹Champalimaud Research, Champalimaud Centre for the Unknown, Lisbon, Portugal. ²Laboratory of Stem Cells and Cancer, Université Libre de **Epider**

Corresponding Authors: Adriana Sánchez-Danés, Champalimaud Research, Champalimaud Center for the Unknown, Avenida Brasília, Lisboa 1400-038, Portugal. E-mail: adriana.sanchezdanes@research.fchampalimaud.org; and Cédric Blanpain, Université Libre de Bruxelles (ULB), 808, route de Lennik, Bat GE, G2 4.205, Bruxelles 1070, Belgium. E-mail: Cedric.Blanpain@ulb.be

Cancer Discov 2025;15:427-43

doi: 10.1158/2159-8290.CD-24-0263

© 2024 American Association for Cancer Research

RESULTS

Survivin Is Expressed in SmoM2-Expressing Epidermal SCs

As previously shown, the overexpression of *SmoM2* in epidermal SCs using *Krt14-CREER* leads to BCC formation, whereas *SmoM2* expression in epidermal Ps using *Inv-CREER* leads to lesions that are frozen in the preneoplastic stages and fail to progress into invasive BCC (Fig. 1A; ref. 2). To identify the molecular changes associated with *SmoM2* expression in SCs and Ps, we performed bulk RNA sequencing (RNA-seq) of FACS-isolated oncogene-expressing (SmoM2-YFP+) basal cells (β4-integrin high) 8 weeks after tamoxifen administration in *Krt14-CREER/SmoM2-YFP* (SCs enriched, hereafter referred to as *Krt14/SmoM2*) and *Inv-CREER/SmoM2-YFP* (Ps enriched, hereafter referred to as *Inv/SmoM2*).

Bruxelles (ULB), Brussels, Belgium. ³Pharmacy Department, University of Genoa, Genoa, Italy. ⁴Department of Medicine, Centre for Blood Research, Life Sciences Institute, University of British Columbia, Vancouver, Canada.

 $S.\ Canato, R.\ Sarate, and\ S.\ Carvalho-Marques\ share\ co-first\ authorship.$

A. Sánchez-Danés and C. Blanpain share co-last authorship.

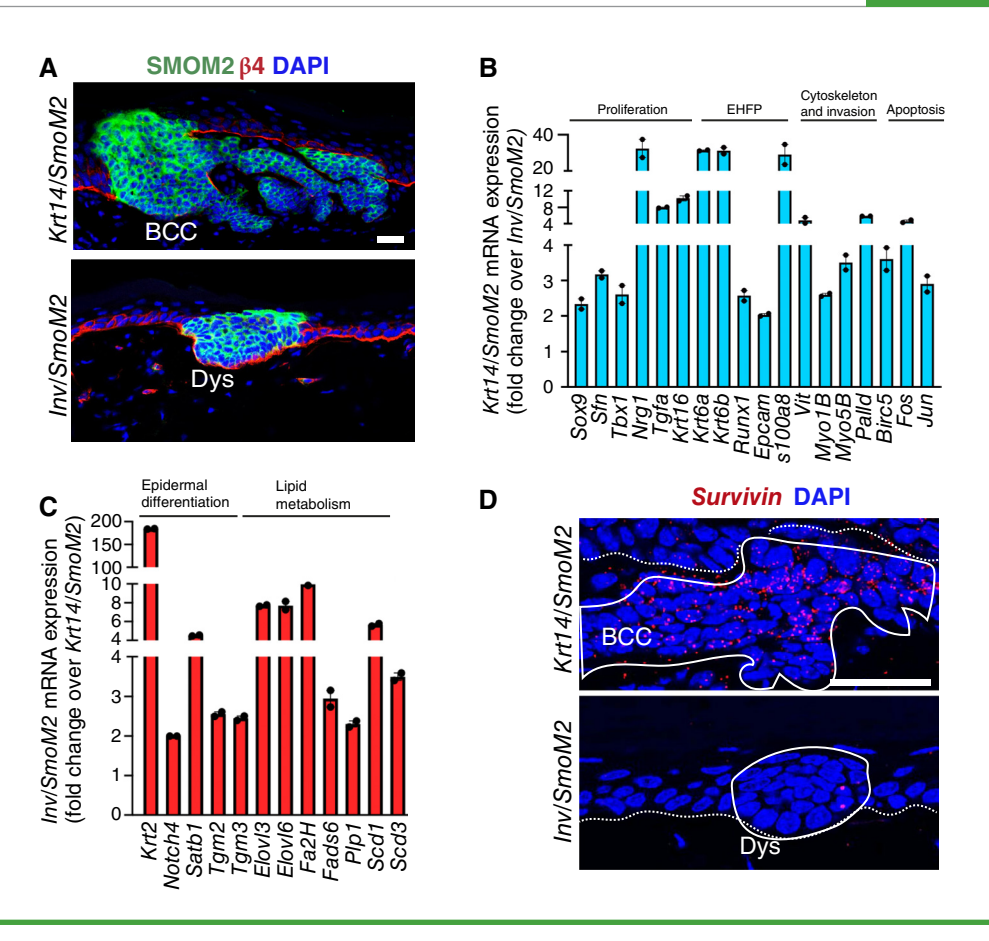


Figure 1. Survivin expression in SCs and Ps after SmoM2 expression. **A,** Image of tail skin section showing immunostaining for β4-integrin and SMOM2 in Krt14/SmoM2 and Inv/SmoM2 mice at 8 weeks after tamoxifen administration. **B,** mRNA expression of genes upregulated in SmoM2-expressing SCs compared with SmoM2-expressing Ps as defined by RNA-seq (n = 2, mean \pm SEM). **C,** mRNA expression of genes upregulated in SmoM2-expressing Ps compared with SmoM2-expressing SCs as defined by RNA-seq (n = 2 mean \pm SEM). **D,** RNA FISH for SmoM2-expressing SCs and Ps. Scale bar, SmoM2-expressing SCs and Ps.

Oncogene-expressing SCs upregulated genes were associated with SC proliferation (e.g., Sox9), stemness (e.g., Tbx1; refs. 8, 9), keratinocyte proliferation (e.g., Nrg1, Tgfa, Krt6a, and Krt16; refs. 10–12), embryonic hair follicle progenitors (e.g., Runx1; ref. 5), and cytoskeleton and invasion (e.g., Myo1B, Myo5B, and Palld; Fig. 1B; ref. 8). In addition, genes negatively regulating apoptosis (e.g., Birc5, Fos, and Jun; refs. 13, 14) were also enriched in Krt14/SmoM2-expressing cells (Fig. 1B). By contrast, the Inv/SmoM2-expressing cells were enriched for genes involved in epidermal differentiation (e.g., Notch4, Satb1, Tgm2, and Tgm3) and lipid metabolism and lipid synthesis (e.g., Elov13, Elov16, Fa2h, Fads6, and Scd1; Fig. 1C), as previously described in Inv-CREER/Rosa-YFP cells (1).

Among the genes downregulated in Ps expressing *SmoM2*, *Birc5* also known as *Survivin* attracted our attention, as the Ps present increased apoptosis compared with SCs after *SmoM2* expression (2). Survivin is a member of the inhibitors of apoptosis protein family that are also involved in the control of mitosis, as it is a part of the chromosomal passenger complex and is expressed in several cancer types (14). *In situ* hybridization (ISH) confirmed high levels of *Birc5/Survivin* expression in BCCs derived from *Krt14/SmoM2* mice when compared with low levels observed in *Inv/SmoM2*-derived dysplasia (Fig. 1D).

These data suggest that the upregulation of *BircS/Survivin* in oncogene-expressing SCs but not in Ps could regulates the competence of SCs to initiate BCC development.

Survivin Deletion in SCs Prevents BCC Formation

To assess whether Survivin expression in SCs is required for BCC development, we performed conditional deletion of Survivin together with the activation of SmoM2 in SCs using Krt14-CREER/SmoM2/Survivinfl/fl (referred to hereafter as SmoM2/Survivin cKO) mice in which Survivin deletion was induced together with activation of oncogenic SmoM2 after tamoxifen administration (Fig. 2A; Supplementary Fig. S1A). The persistence of oncogene-expressing cells and the pathological phenotype (hyperplasia, dysplasia, and invasive BCC) of oncogene-expressing cells was assessed by confocal microscopy on whole mount of tail epidermis (2). Deletion of Survivin in SmoM2/Survivin cKO mice lead to a strong decrease in tumor burden and a rapid loss of oncogeneexpressing cells (Fig. 2B-D; Supplementary Fig. S1B and S1C). By contrast, in the presence of Survivin in Krt14/ SmoM2 mice, most of the clones expressing SmoM2 survived over time and progressed into BCC as previously described

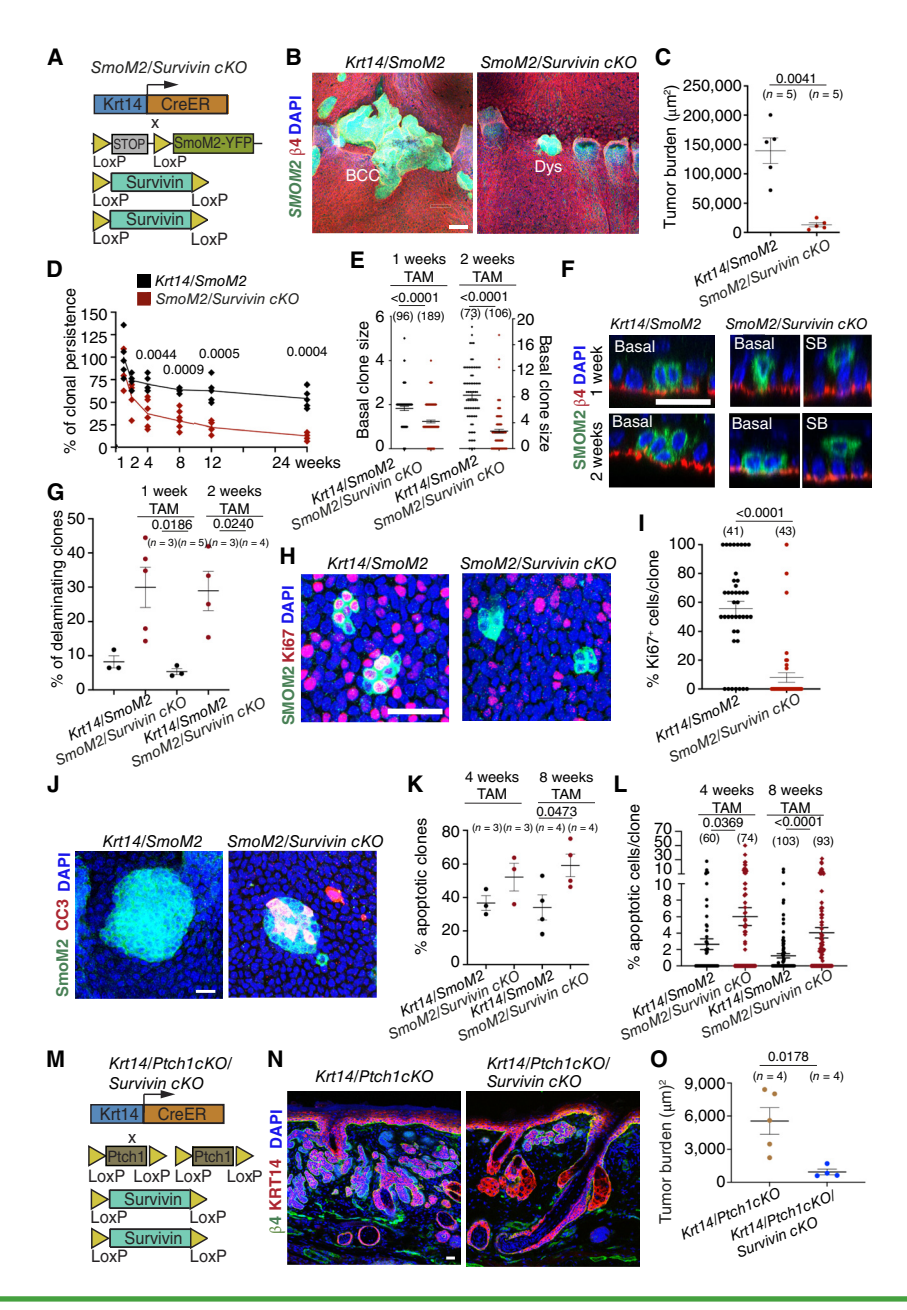


Figure 2. Survivin deletion in SCs prevents BCC formation. A, Genetic strategy to activate SmoM2 expression and delete Survivin in epidermal SCs. **B**, Confocal analysis of immunostaining for SmoM2 and β4-integrin on whole mounts of tail skin of Krt14/SmoM2 and SmoM2/Survivin cKO mice at 12 weeks after tamoxifen administration. C, Quantification of tumor burden defined by the area occupied by SmoM2 tumorigenic lesions in a skin surface area comprising six groups of triplets of hair follicles in Krt14/SmoM2 and SmoM2/Survivin cKO mice 12 weeks after tamoxifen administration (n = number of mice). Statistical analysis was determined using the Welch t test. D. Quantification of the clonal persistence in the interscale region of Krt14/SmoM2 and SmoM2/ Survivin cKO mice at different times of tamoxifen administration of at least n = 5 animals per time point/genotype. Statistical analysis was determined using two-way ANOVA. **E,** Basal clone size in Krt14/SmoM2 and SmoM2/Survivin cKO mice at 1 and 2 weeks after tamoxifen administration (n = clones quantified from at least three different animals). Statistical analysis was determined using the Mann-Whitney test. F, Confocal analysis of immunostaining for SmoM2 and β4-integrin in Krt14/SmoM2 and SmoM2/Survivin cKO mice at 1 and 2 weeks after tamoxifen administration. Orthogonal view was used to quantify the number of basal and suprabasal cells per clone. G, Percentage of clones presenting only suprabasal cells (delaminating/differentiating clones) in Krt14/SmoM2 and SmoM2/Survivin cKO mice at 1 and 2 weeks after tamoxifen administration (n = animals analyzed). Statistical significance was assessed using the Welch t test. **H,** Immunostaining for Ki67 and SmoM2 at 2 weeks after tamoxifen administration in Krt14/SmoM2 and $SmoM2/Survivin\,cKO$ mice. I, Percentage of Ki67* cells per clone at 2 weeks after SmoM2 activation in Krt14/SmoM2 and SmoM2/Survivin cKO mice (n = clones quantified from two different animals). Statistical significance was assessed using the Mann-Whitney test. J, Immunostaining for CC3 and SmoM2 at 8 weeks after tamoxifen administration in Krt14/SmoM2 and SmoM2/Survivin cKO mice. K, Quantification of the number of apoptotic clones at 4 and 8 weeks after SmoM2 activation in Krt14/SmoM2 and SmoM2/Survivin cKO mice (n = number of mice). Statistical significance was assessed using the Welch t test. L, Quantification of the number of apoptotic cells per clone at 4 and 8 weeks after SmoM2 activation in Krt14/SmoM2 and SmoM2/Survivin cKO mice (n = clones quantified from at least three different animals). Statistical significance was assessed using the Mann-Whitney test. M, Genetic strategy to delete both Ptch1 and Survivin in SCs. N, Image of ventral skin sections showing immunostaining for KRT14 and β4-integrin in Krt14/Ptch1cKO and Krt14/Ptch1cKO/Survivin cKO mice at 12 weeks after tamoxifen administration. **0,** Tumor burden in Krt14/Ptch1cKO and Krt14/Ptch1cKO/Survivin cKO mice (n = mice). Statistical significance was assessed using the Welch t test. Error bars represent the mean ± SEM in each figure. Scale bar, 50 µm in **B**, 20 µm in **F**, **H**, and **J**, and 20 µm in **N**.

(Fig. 2B–D; Supplementary Fig. S1B and S1C; ref. 2). Only some of the rare persisting oncogene-expressing clones in *SmoM2/Survivin cKO* mice progressed into small BCCs, accounting for around 6% of the initially induced clones compared with the 21% in *Krt14/SmoM2* mice 12 weeks after tamoxifen administration (Fig. 2D; Supplementary Fig. S1B and S1C). These rare small BCCs found in the *SmoM2/Survivin cKO* mice expressed SURVIVIN as demonstrated by immunostaining for SURVIVIN expression and *Survivin* ISH, indicating that the small fraction of BCC arising in *SmoM2/Survivin cKO* mice correspond to escaper cells that did not recombine and delete *Survivin* floxed alleles (Supplementary Fig. S1D and S1E).

To understand the causes of the loss of oncogene-expressing cells after Survivin deletion, which could be already observed 1 week after tamoxifen administration, we first assessed the basal clone size. We observed that the Krt14/SmoM2 clones presented more basal cells (1.8 vs. 1.2 cells per clone) by 1 week after tamoxifen administration and 6.6 versus 2.1 cells per clone by 2 weeks when compared with SmoM2/Survivin cKO (Fig. 2E). In addition, upon Survivin deletion, around 30% of the clones by weeks 1 and 2 did not have basal attachment, indicating that these cells were differentiating, leading to delamination and clone loss (Fig. 2F and G). By contrast, only 8% and 4% of the Krt14/SmoM2 clones expressing Survivin were delaminating at 1 and 2 weeks, respectively. Immunostaining for SmoM2 and the differentiation marker keratin 10 (KRT10) 2 weeks after tamoxifen administration showed a higher number of SmoM2 basal cells expressing KRT10 after Survivin deletion (Supplementary Fig. S1F and S1G). In Krt14/SmoM2 clones, KRT10 was expressed in suprabasal layers, whereas SURVIVIN was expressed in the proliferative basal compartment, as shown by colocalization of SURVIVIN with AURORA KINASE B, a protein required in chromosome segregation and cytokinesis (Supplementary Fig. S1H and S1I; ref. 15).

In addition, cell proliferation was strongly decreased after *Survivin* deletion, as shown by the decrease in Ki67⁺ cells (56% and 8% of Ki67⁺ cells in *Krt14/SmoM2* and *SmoM2/Survivin cKO* mice) at 4 weeks after tamoxifen administration (Fig. 2H and I).

To assess whether, in addition to the promotion of differentiation and delamination, an increase of apoptosis after *Survivin* deletion (14) participates in the loss of oncogene-expressing clones, we quantified the proportion of cleaved caspase-3 (CC3)-expressing cells in the presence and absence of *Survivin* after *SmoM2* expression. We found that *Survivin* deletion strongly increased the number of clones that were positive for CC3 and the proportion of apoptotic cells per clone from 2.6% to 6% by 4 weeks after tamoxifen administration and from 1.2% to 4% by 8 weeks after tamoxifen administration in *Krt14/SmoM2* and *SmoM2/Survivin cKO* mice, respectively. (Fig. 2J-L). We did not observe cells co-expressing CC3 and SURVIVIN in lesions from *Krt14/SmoM2* mice (Supplementary Fig. S1J).

The most prevalent mutation leading to BCC in humans is the loss of function of the tumor suppressor gene *Ptch1* (4). To assess if the key role of *Survivin* in promoting the survival of *SmoM2*-expressing cells is conserved across different mutations promoting oncogenic Hh signaling, we performed conditional

deletion of *Ptch1* and *Survivin* in *Krt14-CREER/Ptch1^{fl/fl}/Survivin^{fl/fl}* mice (hereafter referred to as *Krt14/Ptch1cKO/SurvivincKO*; Fig. 2M). Similar to what we found in *SmoM2* mice, we found that deletion of *Survivin* in the context of *Ptch1* deletion also strongly inhibited the formation of BCC (Fig. 2N and O). Altogether, these data indicate that *SURVIVIN* expression in SCs is critically important for BCC formation by promoting oncogene-expressing cell proliferation and survival through the restriction of apoptosis and terminal differentiation.

Survivin Overexpression Confers to Ps the Competence to Initiate BCC Development

As the survival of SmoM2-targeted cells in Ps and SCs after the loss of function of Survivin decreases over time, we assessed whether the gain of function of Survivin could rescue the survival of SmoM2-expressing Ps and render the Ps competent to initiate BCC formation. To this end, we generated a new genetic mouse model allowing the overexpression of Survivin in the basal cells targeted by SmoM2 in a doxycycline inducible manner (Supplementary Materials and Methods; Supplementary Fig. S2A and S2B). In this new genetic model, cells that overexpress Survivin could be identified by mCHERRY expression because of the presence of a Survivin-IRES-mCherry cassette (Supplementary Fig. S2A and S2B). To test the effect of *Survivin* overexpression in Ps upon oncogenic activation, we generated the Inv-CREER/Rosa-SmoM2-YFP/Krt14rtTA/ tetO-Survivin-IRES-mCherry, hereafter referred to as Inv/SmoM2/ Survivin GOF (Fig. 3A). Specifically, the Inv/SmoM2/Survivin GOF mice were treated with doxycycline to overexpress Survivin starting for the duration of the experiment and 1 week before tamoxifen administration, the latter leading to SmoM2 expression (Supplementary Fig. S2C).

Upon Survivin overexpression, the oncogene-targeted Ps gave rise to BCCs, with 12% and 26% of the clones being BCCs at 8 and 12 weeks after SmoM2 expression, respectively. In the absence of Survivin overexpression, oncogene-targeted Ps did not progress from dysplasia into BCCs as previously reported (Fig. 3B-D; Supplementary Fig. S2D; ref. 2). In addition, Survivin overexpression led to stabilization in the survival of oncogene-targeted cells after the second week subsequent to oncogene expression, although the number of clones in SmoM2-targeted Ps continued to decrease over time as previously described (Fig. 3E; Supplementary Fig. S2E; ref. 2). We did not find differences in the number of proliferative cells or basal clone size in BCCs arising from SCs in the Krt14/ SmoM2 model compared with BCCs arising from Ps upon Survivin and SmoM2 expression in Inv/SmoM2/Survivin GOF mice (Supplementary Fig. S2F and S2G).

To define the mechanisms by which *Survivin* overexpression confers competence of Ps to induce clonal persistence and BCC formation, we first assessed whether *Survivin* overexpression promotes clonal expansion in oncogene-targeted Ps. We found that *Survivin* overexpression led to an increase in basal clone size at different time points after oncogene expression (Fig. 3F). We then assessed whether *Survivin* overexpression prevented the elimination of oncogene-targeted Ps by apoptosis (2). Upon *Survivin* overexpression, the proportion of clones expressing CC3 decreased as did the percentage of CC3-positive cells per clone 8 weeks after tamoxifen

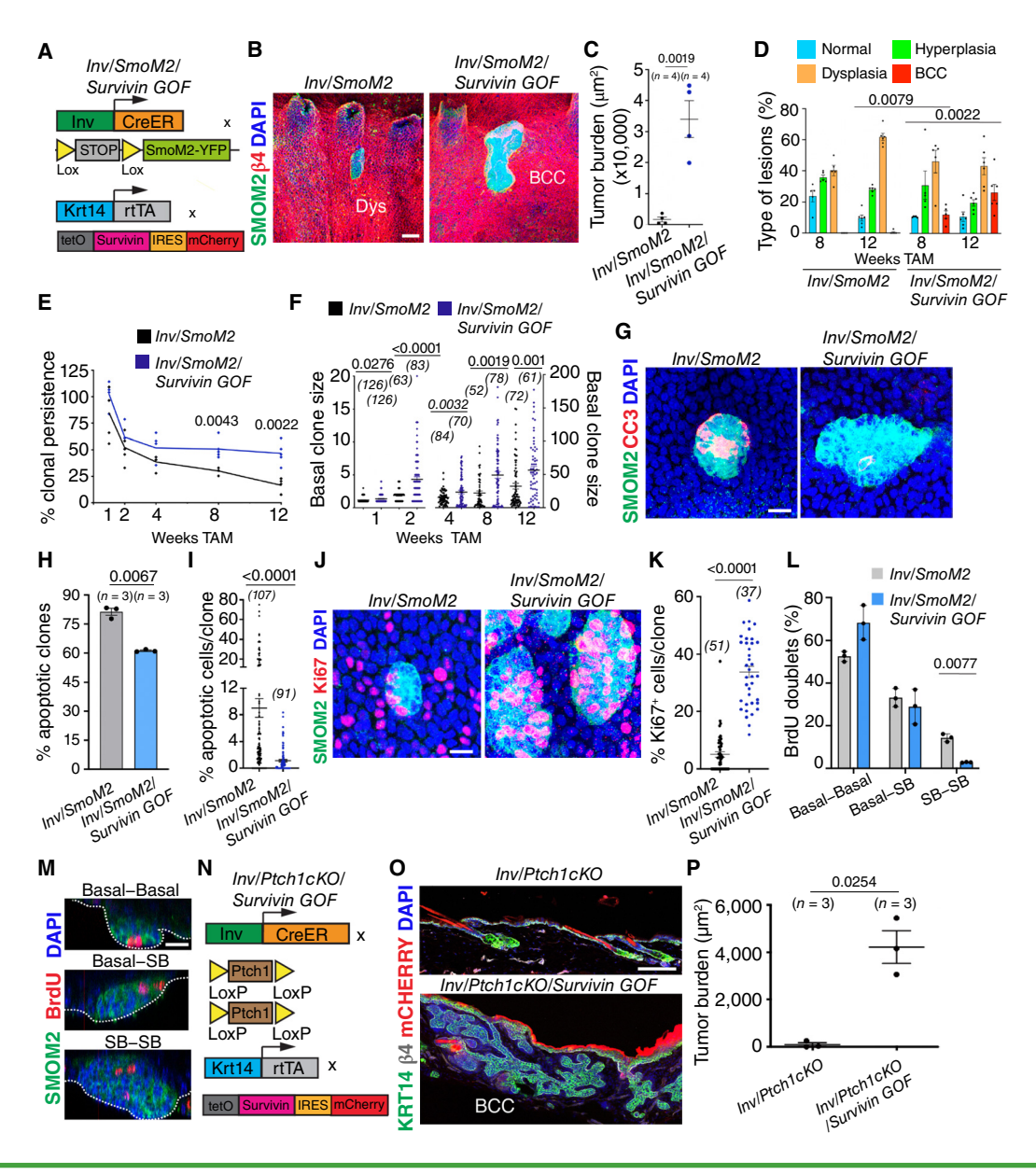


Figure 3. Survivin overexpression in Ps confers the competence for BCC initiation. A, Genetic strategy to activate SmoM2 and overexpress Survivin in Ps. B, Confocal analysis of immunostaining for SmoM2 and β4-integrin on whole mounts of tail skin from Inv/SmoM2 and Inv/SmoM2/Survivin GOF mice at 12 weeks after tamoxifen administration. C, Tumor burden in Inv/SmoM2 and Inv/SmoM2/Survivin GOF mice at 12 weeks after tamoxifen administration. (n = number of mice). Statistical significance was assessed using the Mann-Whitney test. **D**, Quantification of the lesion morphology in Inv/SmoM2 and Inv/SmoM2/Survivin GOF mice at 8 and 12 weeks after tamoxifen administration. (n = number of mice). Statistical significance was assessed using the Mann-Whitney test E, Quantification of the clonal persistence in the interscale region of Inv/SmoM2 and Inv/SmoM2/Survivin GOF mice at different times of tamoxifen administration of at least n = 5 animals per time point/genotype. Statistical significance was assessed using the Mann–Whitney test. F, Basal clone sizes in Inv/SmoM2 and Inv/SmoM2/Survivin GOF mice at different times of tamoxifen administration (n = clones from two mice). Statistical significance was assessed using the Mann-Whitney test. G, Immunostaining for CC3 and SmoM2 at 8 weeks after tamoxifen administration in Inv/SmoM2 and Inv/ SmoM2/Survivin GOF mice. H, Quantification of the number of apoptotic clones at 8 weeks after tamoxifen administration in Inv/SmoM2 and Inv/SmoM2/ Survivin GOF mice (n = 3 mice). Significance was determined using the Welch t test. I, Quantification of the number of apoptotic cells per clone at 8 weeks after tamoxifen administration in Inv/SmoM2 and Inv/SmoM2/Survivin GOF mice (n = clones analyzed from three different animals). Statistical significance was assessed using the Mann-Whitney test. J, Confocal analysis of immunostaining for SmoM2 and β4-integrin on whole mounts of tail skin of Inv/SmoM2 and Inv/SmoM2/Survivin GOF mice at 8 weeks after tamoxifen administration. K, Percentage of Ki67+ cells per clone at 2 weeks after SmoM2 activation in Inv/SmoM2 and Inv/SmoM2/Survivin GOF mice (n = clones from three mice). Significance was determined using the Mann-Whitney test. L, BrdU short-term lineage tracing to define cell fate outcome of progenitors (BrdU doublets) in Inv/SmoM2 and Inv/SmoM2/Survivin GOF mice at 8 weeks (n = 3 mice/group). Statistical significance was assessed using the Welch t test. M, Short-term fate outcome of progenitors in Inv/SmoM2/Survivin GOF clones at 8 weeks, as assessed by using BrdU as a clonal marker. Only cell doublets were counted and classified as basal-basal, basal-suprabasal (SB), or SB-SB. Immunostaining for BrdU and SmoM2 showing the different types of cell fate outcomes found in Inv/SmoM2/Survivin GOF clones. N, Genetic strategy to delete Ptch1 and overexpress Survivin in Ps. 0, Image of ventral skin sections showing immunostaining for KRT14 and β4-integrin and endogenous expression of mCHERRY in Inv/Ptch1cKO and Inv/Ptch1cKO/Survivin GOF mice at 12 weeks after tamoxifen administration. P, Tumor burden in Inv/Ptch1cKO and Inv/Ptch1cKO and Inv/Ptch1cKO/Survivin GOF mice at 12 weeks after tamoxifen administration (n = number of mice). Statistical significance was assessed using the Welch t test. Error bars represent the mean ± SEM in each figure. Scale bar, 50 µm in **B**, 20 µm in **G**, **J**, and **M**, and 200 µm in **O**. Number of clones counted presented in parentheses.

administration (Fig.3G–I). Next, we assessed if this increase in clone size could be also mediated by a difference in cell proliferation. To this end, we assessed oncogene-targeted cell proliferation by quantifying the number of proliferative cells per clone. We found an increase in Ki67+ cells after *Survivin* overexpression in the *Inv/SmoM2/Survivin* GOF clones compared with *Inv/SmoM2*, indicating that proliferation was enhanced after *Survivin* overexpression (Fig. 3J and K).

To assess whether clonal survival and BCC formation after Survivin overexpression was the consequence of a change in cell fate outcome favoring symmetric cell division, we performed short-term 5-bromo-2'-deoxyuridine (BrdU) pulse chase experiments. To this end, we administrated a low dose of BrdU to mark a minority of dividing cells and assessed the cell fate outcome 3 days later by quantifying the relative proportion of basal and suprabasal localization of BrdU doublets. We found that Survivin overexpression in SmoM2-expressing Ps led to an increase in the proportion BrdU doublets made of two basal cells (from 52% in Inv/SmoM2 to 68% in Inv/SmoM2/ Survivin GOF) and a decrease in divisions that led to doublets of differentiated cells (from 14% in Inv/SmoM2 to 3% in Inv/ SmoM2/Survivin GOF). This data indicates that Survivin overexpression in SmoM2-expressing Ps promotes self-renewing divisions and prevents cell differentiation, similar to what we have found in SmoM2-expressing SCs (Fig. 3L and M; ref. 2). Survivin overexpression in wild-type skin did not lead to the formation of BCC or alter the differentiation potential of the basal cells of the epidermis (Supplementary Fig. S2H and S2I).

We then assessed whether the promotion of BCC formation by *Survivin* overexpression in Ps is also found after *Ptch1* deletion. To this end, we generated *Inv-CREER/Ptch1* fl.fl.fkrt14-rtta/teto-Survivin-IRES-mCherry mice (hereafter referred to as *Inv/Ptch1cKO/Survivin GOF*; Fig.3N). Survivin overexpression also led to BCC formation arising from the Inv-targeted Ps after *Ptch1* deletion (Fig.3O and P), demonstrating that the promotion of BCC formation by *Survivin* overexpression in Ps is conserved across different oncogenic mutations activating Hh pathway.

Altogether these data indicate that *Survivin* overexpression confers the competence of oncogene-targeted Ps to initiate BCC formation by enhancing proliferation and promoting self-renewing divisions, as well as by inhibiting apoptosis and preventing differentiation in preneoplastic lesions arising from Ps.

Survivin Promotes Stem Cell-like Properties during Skin Homeostasis

To determine whether *Survivin* expression controls stemness in skin SCs in the absence of oncogene expression, we first assessed whether *Survivin* is upregulated in normal SCs compared with Ps. qRT-PCR showed that *Survivin* expression is upregulated in homeostatic SCs (*Krt14-CREER/Rosa-YFP* clones, hereafter referred to as *Krt14/YFP*) compared with Ps (*Inv-CREER/Rosa-YFP* clones, hereafter referred to as *Inv/YFP*) in homeostatic conditions (Supplementary Fig. S3A).

Using the gain and loss of functions of *Survivin*, we assessed whether *Survivin* expression controls stemness in skin SC *in vivo* during homeostatic conditions. Deletion of *Survivin* together with the expression of reporter gene YFP in SCs

using Krt14 promoter in Krt14-CREER/Rosa-YFP/Survivin^{fl/fl} mice, hereafter referred to as Krt14/YFP/Survivin cKO (Supplementary Fig. S3B), led to an increase in clonal loss over time compared with clones expressing wild-type Survivin (Krt14-CREER/Rosa-YFP mice) from 62.8% to 20.2% by 12 weeks after tamoxifen administration (Supplementary Fig. S3C and S3D). The Krt14/YFP clones that persisted were bigger than the clones of Krt14/SmoM2/Survivin cKO (3.4 basal cells vs. 2.4 basal cells) at 12 weeks after tamoxifen administration (Supplementary Fig. S3E).

By contrast, the overexpression of *Survivin* in Ps in a homeostatic condition using the *Inv-CREER/Rosa-YFP/Krt14rtTA/tetO-Survivin-IRES-mCherry*, referred to as *Inv/YFP/Survivin GOF* (Supplementary Fig. S3F and S3G), led to an increase in clonal persistence from 8.1% to 30% and an increase in clone size (basal cells 2.5 in wild-type vs. 3.6 basal cells upon *Survivin* overexpression) at 12 weeks after tamoxifen administration (Supplementary Fig. S3H–S3J). These data show that *Survivin* deletion in SCs leads to a clonal behavior similar to Ps, whereas the overexpression of *Survivin* in Ps leads to a clonal behavior similar to SCs, indicating that *Survivin* mediates stemness in the skin basal compartment in the absence of oncogene expression.

Pharmacologic Inhibition of Survivin Prevents the Progression of Preneoplastic Lesions into BCCs

To define the role of *Survivin* expression during the progression of preneoplastic lesions into invasive BCCs, we first assessed Survivin expression in hyperplasia and dysplasia derived from SCs and Ps. Survivin was highly expressed at the mRNA and protein levels in hyperplasia and dysplasia derived from SCs in the Krt14/SmoM2 mice compared with lesions derived from Ps in the *Inv/SmoM2* mice (Supplementary Fig. S4A and S4B). To test whether Survivin can promote the conversion of preneoplastic lesions into invasive BCCs in Krt14/ SmoM2 and Inv/SmoM2/Survivin GOF mice, we treated mice with Survivin inhibitor (YM155) at 8 weeks after tamoxifen administration (Fig. 4A), a time point when the majority of lesions are dysplasia that progress into BCC (Fig. 3D; Supplementary Fig. S1C). We could only treat the mice for 10 days, as long-term administration of this inhibitor induces systemic toxicity that requests the termination of the experiments. Treatment of Krt14/SmoM2 and Inv/SmoM2/Survivin GOF mice with Survivin inhibitor led to a decrease in the number of lesions and tumor burden, and also to a decreased number of lesions that progressed into BCC from around 60% to 20% in Krt14/SmoM2 mice and from 45% to less than 10% in the Inv/SmoM2/Survivin GOF mice (Fig. 4B-D; Supplementary Fig. S4C and S4D). To define the underlying mechanisms that restrict the progression of these preneoplastic lesions into BCCs, we performed immunostaining for markers of apoptosis (CC3) and proliferation (Ki67) upon Survivin inhibitor administration. We observed an increase in apoptosis from 0.3% to 11.37% of CC3+ in Krt14/SmoM2 and from 3.5% to 17.4% in Inv/SmoM2/Survivin GOF after inhibitor administration (Fig. 4E-G). In addition, administration of Survivin inhibitor decreased proliferation from 35.7% of Ki67+ cells to 23.3% in Krt14/SmoM2 mice and from 15.2% to 7.8% in Inv/SmoM2/ Survivin GOF mice (Fig. 4H and I). In addition, immunostaining

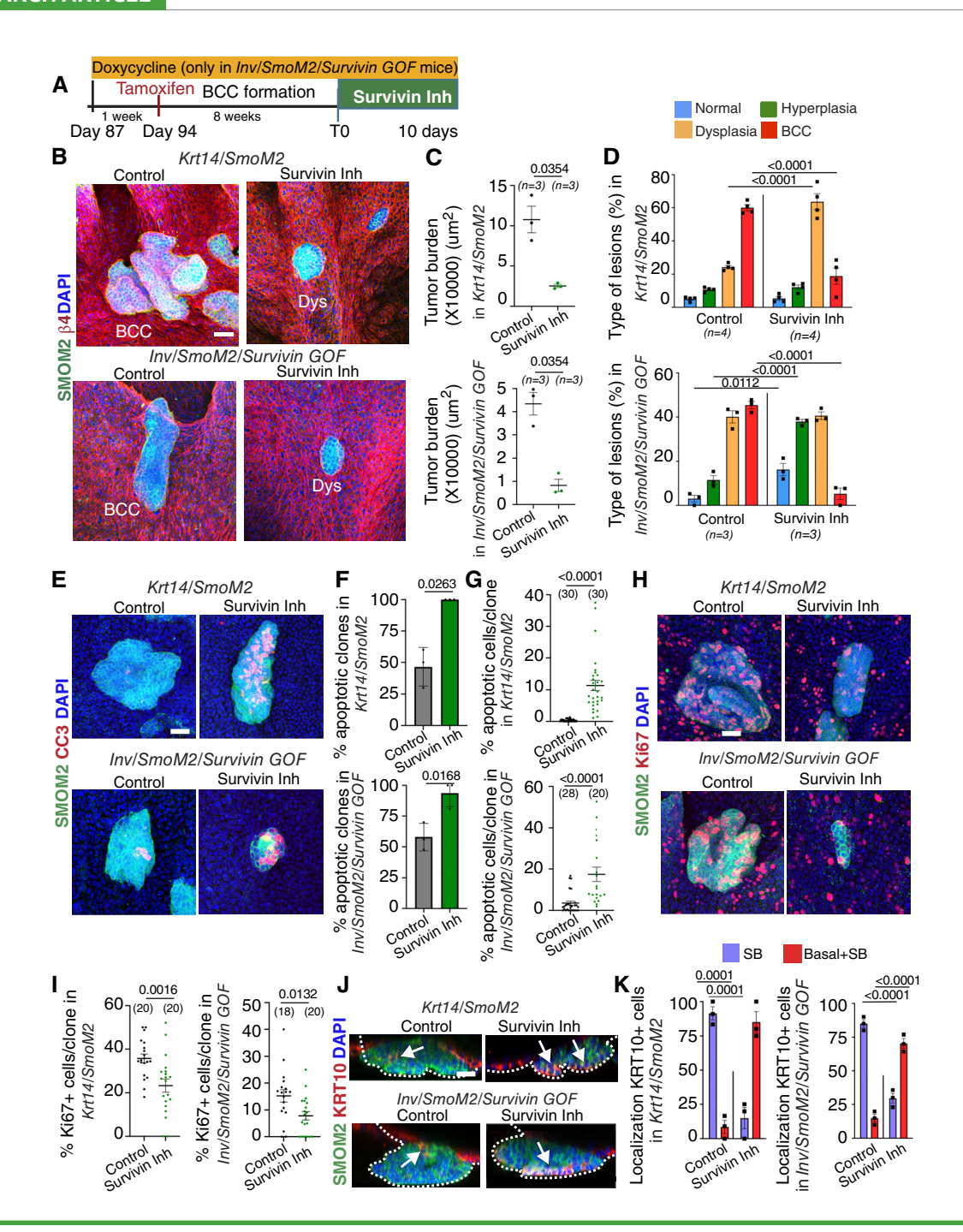


Figure 4. Survivin inhibitor treatment prevents the conversion of preneoplastic lesions into BCCs. A, Protocol for tumor induction and Survivin inhibitor treatment. **B**, Confocal analysis of immunostaining for SmoM2 and β 4-integrin on whole mounts of tail skin of Krt14/SmoM2 and Inv/SmoM2/SurvivinGOF mice at the end of the Survivin inhibitor treatment. C, Tumor burden Krt14/SmoM2 and Inv/SmoM2/Survivin GOF mice at the end of the Survivin inhibitor treatment. (n = number of mice). Statistical significance was assessed using Mann-Whitney test. D, Quantification of the lesion morphology in Krt14/SmoM2 and Inv/SmoM2/Survivin GOF mice at the end of the Survivin inhibitor treatment and control (n = mice). Statistical significance was assessed using the Mann-Whitney test. E, Immunostaining for CC3 and SmoM2 after Survivin inhibitor treatment in Krt14/SmoM2 and Inv/SmoM2/ Survivin GOF mice. F. Quantification of the number of apoptotic clones at the end of the Survivin inhibitor treatment in Krt14/SmoM2 and Inv/SmoM2/ Survivin GOF mice. (n = 3 mice/group) Significance was determined using the Welch t test. G, Quantification of the number of apoptotic cells per clone at the end of the Survivin inhibitor treatment in Krt14/SmoM2 and Inv/SmoM2/Survivin GOF mice. (n = clones analyzed from three to two different animals in Krt14/SmoM2 and Inv/SmoM2/Survivin GOF, respectively). Statistical significance was assessed using the Mann-Whitney test. H, Confocal analysis of immunostaining for SmoM2 and Ki67 on whole mounts of tail skin of Krt14/SmoM2 and Inv/SmoM2/Survivin GOF mice at the end of the Survivin inhibitor treatment. I, Percentage of Ki67+ cells per clone at the end of the Survivin inhibitor treatment in Krt14/SmoM2 and Inv/SmoM2/Survivin GOF mice (n = clones from two mice). Significance was determined using the Mann-Whitney test. **J,** Immunostaining for SmoM2 and KRT10 in Krt14/SmoM2 and Inv/SmoM2/Survivin GOF lesions at the end of the Survivin inhibitor treatment. K, Quantification of the tumorigenic lesions from Krt14/SmoM2 and Inv/SmoM2/Survivin GOF mice containing KRT10 in suprabasal (SB) or basal + SB layers (n = 3 mice/group). Error bars represent the mean ± SEM in each figure. Scale bar, 50 µm in B, 20 µm in E, H, and J. Number of clones counted presented in parentheses.

for the differentiation marker KRT10 showed that in the untreated tumorigenic lesions, KRT10 was mainly observed in suprabasal differentiated cells and that the treatment with Survivin inhibitor led to the expression of KRT10 in basal cells (Fig. 4J and K). Altogether, these results indicate that administration of Survivin inhibitor decreases the progression of the preneoplastic lesions into BCC by promoting apoptosis and differentiation, as well as decreasing proliferation.

To determine whether overexpression of Survivin in SmoM2-expressing preneoplastic lesions derived from Ps allow them to progress into BCC, we administrated tamoxifen to activate SmoM2 in Ps in Inv/SmoM2/Survivin GOF mice. Three weeks after tamoxifen administration when the majority of the lesions became hyperplasia and some became dysplasia, we administered doxycycline to overexpress Survivin (Supplementary Fig. S4E). After Survivin overexpression, 20% of the lesions progressed into BCC at 8 weeks after tamoxifen administration, compared with 0% in the absence of Survivin overexpression (Fig. 3D; Supplementary Fig. S4F-S4H), which is similar to the proportion of BCCs observed when Survivin is overexpressed before tamoxifen administration (Supplementary Figs. S1C and S4H). However, the total number of clones was reduced by 50% compared with Survivin overexpression prior to tamoxifen administration (Supplementary Fig. S4I). These results further confirm that Survivin overexpression promotes progression of preneoplastic lesions into BCC.

Survivin Overexpression Prevents Ps Differentiation into Different Epidermal Lineages

As Survivin overexpression confers the competence of Ps to initiate BCC formation after oncogenic Hh mutations by promoting self-renewing divisions and restricting apoptosis and differentiation, we next assessed whether the cell state changes induced by SmoM2 expression in Ps is affected by Survivin overexpression. To this end, we performed single-cell RNA-seq (scRNA-seq) on FACS-isolated SmoM2-YFP cells from Inv/SmoM2 (n = 8,046 cells) and Inv/SmoM2/SurvivinGOF (n = 6,056 cells) mice 8 weeks after tamoxifen administration. We performed unsupervised clustering on individual samples using Seurat and annotated different clusters based on known genes expressed for each condition previously described by scRNA-seq of skin epidermis (16-19). In both conditions, we identified different clusters based on the expression of specific genes that can be classified into distinct SC/P clusters, SC/P G₀ (e.g., Igfbp2, Stfa3, and Sparc), SC/P G₂-M (e.g., Mki67, Top2a, and Cenpa), differentiated basal cells of the scale (e.g., Krt36 and Krt84), differentiated basal cells of the interscale (e.g., Krt2 and Krt10), sebaceous glands (SG) (e.g., Mgst1 and Scd1), committed cells (e.g., Krt17, Mt2, and Krtdap), infundibulum progenitor (e.g., Foxc1, Aldh3a1, and Lrig1), infundibulum differentiated cells (e.g., Sox9, Rflnb, and Lmo1), and embryonic hair follicle progenitor reprogramming cells that are found in oncogene-targeted cells during BCC formation (e.g., Lgr5, Lhx2, and Ptch1; Fig. 5A and B; Supplementary Figs. S5A-S5I and S6A-S6I; ref. 5). Our comparative analysis between Inv/SmoM2 and Inv/SmoM2/Survivin GOF showed an increase in the proportion of differentiated cells in the absence of Survivin overexpression (Fig. 5A and B). Data integration

using Seurat showed that Survivin overexpression led to the disappearance of a cell cluster only observed in the *Inv/SmoM2* condition (Fig. 5C and D). Subclustering of this Inv/SmoM2-specific cluster revealed that it was composed by cluster committed toward infundibulum differentiation (e.g., Ly6d and Defb6), cluster committed toward IFE differentiation (e.g., Krt10 and Krtdap), and cluster committed toward SG differentiation (e.g., Scd1 and Mgst1; Fig. 5E and F). To validate the results of scRNA-seq, we performed immunofluorescence (IF) and ISH (RNAscope) analysis using markers specific for the different clusters committed toward differentiation. IF showed that Survivin overexpression restricts the expression of IFE differentiation marker KRT10 and the SG differentiation marker SCD1 in Inv/SmoM2 cells at a similar level as in SmoM2-expressing SCs (Fig. 5G and H). Defb6 ISH revealed that Survivin overexpression restricted the expression of Defb6 in oncogenetargeted Ps, similar to that found in oncogene-targeted SCs (Fig. 5G and H). Altogether these data reveal that Survivin overexpression in oncogene-targeted Ps prevents their differentiation into various epidermal lineages.

Survivin Overexpression Promotes Cell Division and Survival and Prevents Apoptosis and Differentiation

To further refine the molecular mechanisms by which Survivin expression promotes the competence of basal cells to induce BCC formation upon SmoM2 expression, we performed bulk RNA-seq of SCs and Ps in the absence (Ps and SCs Survivin KO) or presence (SCs and Ps Survivin GOF) of Survivin expression. To this end, we FACS-isolated basal cells of the IFE (α6-integrin high and CD34 negative) and excluded the bulge SC (α6-integrin high and CD34 positive) expressing SmoM2 fused to YFP from Inv-SmoM2, Inv/SmoM2/Survivin GOF, Krt14/SmoM2, and SmoM2/Survivin cKO mice and performed bulk RNA-seq in two independent biological samples (Supplementary Fig. S7A and S7B). We compared the transcriptome of these different populations and defined different signatures: (a) the SC-specific signature as genes upregulated in SmoM2-expressing SCs compared with SmoM2-expressing Ps (up Krt14/SmoM2 vs. Inv/Smo), (b) the Survivin-regulated gene signature in Ps as genes upregulated in SmoM2-expressing Ps upon Survivin overexpression versus SmoM2-expressing Ps (up Inv/SmoM2/Survivin GOF vs. Inv/SmoM2), and (c) the Survivin-regulated gene signature in SCs as genes downregulated upon Survivin deletion in SmoM2-expressing SCs compared with SmoM2-expressing SCs (up Krt14/SmoM2 vs. SmoM2/Survivin cKO).

We found that 82 genes were commonly upregulated upon *Survivin* expression (common genes across the three different gene signatures) that were enriched for genes regulating survival and proliferation, including *Tgfa*, *Aqp3*, and *Heg1*; ligands of the ErbB receptors (*Nrg1* or *Hbegf*); members of the MAPK signaling pathway (*Map2K3*, *Map3K14*, and *Map3K6*); or *Sgk1*, encoding a kinase that promotes survival and proliferation and inhibits apoptosis (Fig. 6A–C; ref. 20).

In order to validate that the absence/downregulation of *Survivin* expression is associated with keratinocyte differentiation as demonstrated by our previous scRNA-seq data

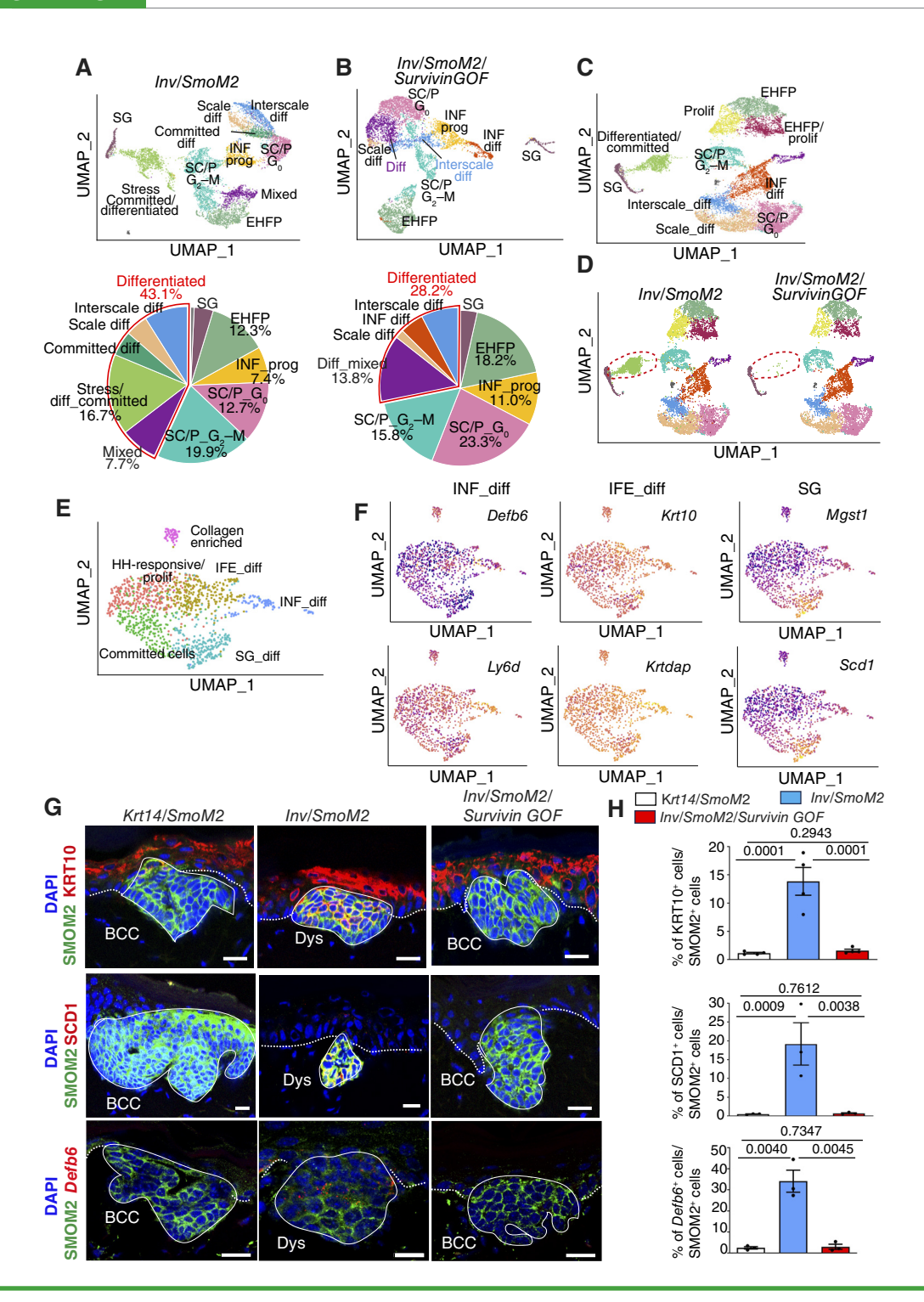


Figure 5. scRNA-seq shows the role of Survivin in preventing keratinocyte differentiation. A and B, Uniform Manifold Approximation and Projection (UMAP) of SmoM2-expressing cells isolated from Inv/SmoM2 mice (A) and Inv/SmoM2/Survivin GOF mice (B) at 8 weeks after tamoxifen administration showing the different cell types and cell states (top) and their relative proportion (bottom). C, UMAP dimensionality reduction plots representing unsupervised clustering: integrated data (Inv/SmoM2 and Inv/SmoM2/Survivin GOF) using Seurat. D, UMAP visualization of SmoM2-expressing cells isolated from Inv/SmoM2 mice and Inv/SmoM2/Survivin GOF mice after data integration. E, Subclustering of the differentiated/committed cluster found in Inv/SmoM2 integrated data is no longer present after Survivin overexpression. F, Cell states found after subclustering of the differentiated/committed cluster found in Inv/SmoM2 integrated data. Color code by normalized gene expression for specific genes for IFE progenitor (Krt10 and Krtdap), infundibulum differentiation (Defb6 and Ly6d), and sebaceous gland (Mgst1 and Scd1). G, Immunostaining for SmoM2-GFP, keratin 10 (KRT10), and SCD1 and ISH for Defb6 in Krt14/SmoM2, Inv/SmoM2/Survivin GOF, and Inv/SmoM2 mice at 8 weeks after tamoxifen administration. H, Quantification of immunostaining for KRT10* cells, SCD1+ cells, and Defb6* cells in SmoM2-expressing clones from Krt14/SmoM2, Inv/SmoM2/Survivin GOF, and Inv/SmoM2 mice at 8 weeks after tamoxifen administration (n = 3 animals/genotype). Significance was determined using the Mann-Whitney test. Error bars represent the mean ± SEM in each figure. Scale bar, 20 μm in G.

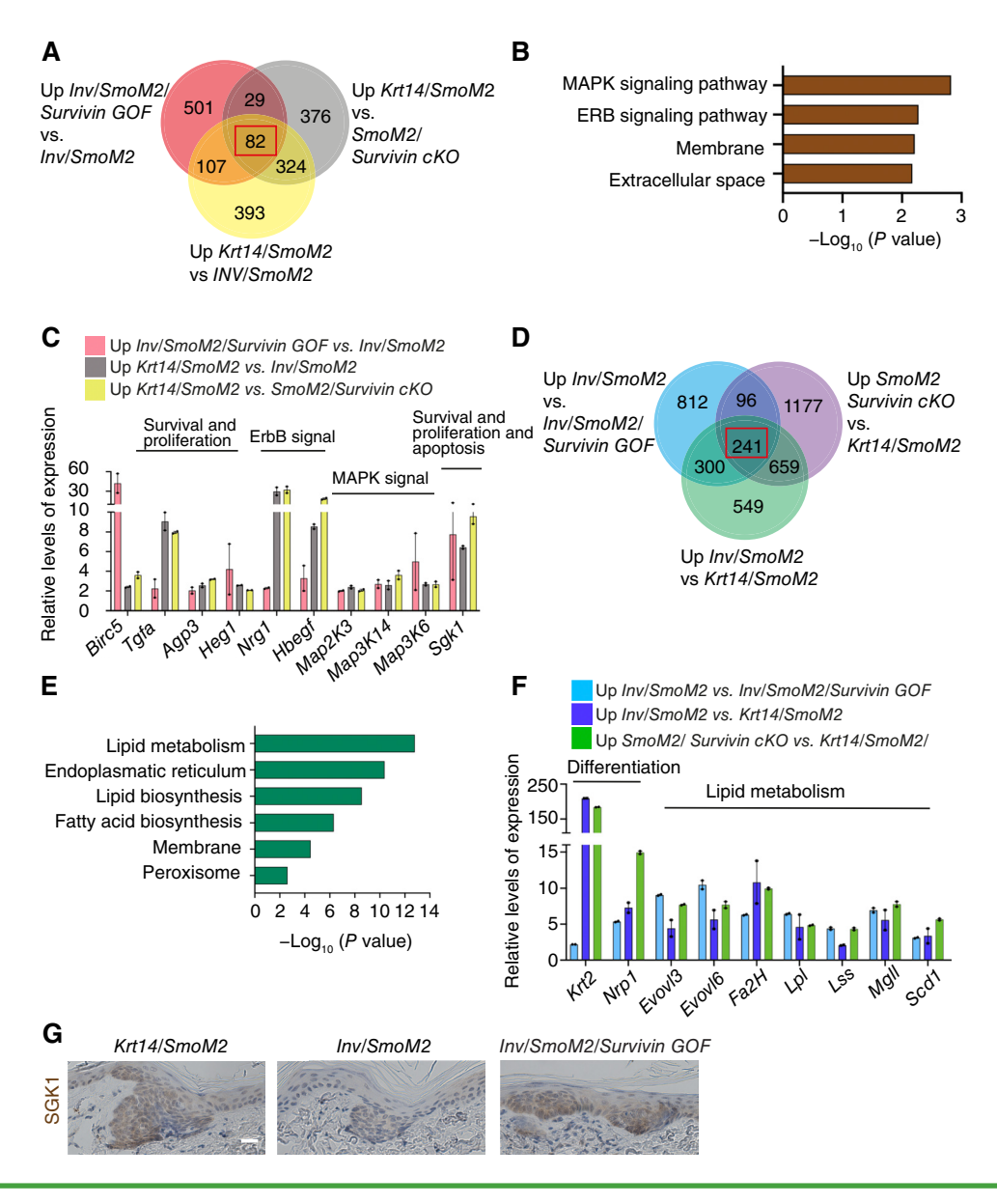


Figure 6. Survivin promotes proliferation and survival and prevents apoptosis and keratinocyte differentiation in SmoM2-expressing cells. **A**, Venn diagram showing the common genes upregulated after Survivin expression in three different conditions: up Krt14/SmoM2 vs. Inv/SmoM2 8 weeks upon tamoxifen administration (yellow), up Inv/SmoM2/Survivin GOF vs. Inv/SmoM2 8 weeks upon tamoxifen administration (pink), and up Krt14/SmoM2 vs. SmoM2/Survivin cKO 6 weeks upon tamoxifen administration (gray). **B**, Gene ontology (GO) analysis of 82 genes upregulated in the three conditions analyzed. **C**, Relative mRNA expression of the genes upregulated in the three conditions analyzed as defined by RNA-seq (n = 2 mean ± SEM). **D**, Venn diagram showing the genes commonly downregulated after Survivin expression in three different conditions: up Inv/SmoM2 vs. Krt14/SmoM2 8 weeks after tamoxifen administration (green), up Inv/SmoM2 vs. Inv/SmoM2/Survivin GOF 8 weeks after tamoxifen administration (blue), and up SmoM2/Survivin cKO vs. Krt14/SmoM2 6 weeks after tamoxifen (purple). **E**, GO analysis of 241 genes downregulated in the three conditions analyzed. **F**, Relative mRNA expression of the genes upregulated in the three conditions analyzed as defined by RNA-seq (n = 2, mean ± SEM). **G**, SGK1 IHC of tail skin sections in Krt14/SmoM2, Inv/SmoM2, and Inv/SmoM2/Survivin GOF mice at 8 weeks after tamoxifen administration.

analysis, we assessed the genes commonly upregulated in the absence of *Survivin* expression in three gene signatures: (d) the P-specific signature as genes upregulated in *SmoM2*-expressing Ps compared with *SmoM2*-expressing SCs (up *Inv/SmoM2* vs. *Krt14/Smo*), (e) the genes upregulated in the absence of *Survivin* expression in the *SmoM2*-expressing Ps (up *Inv/SmoM2* vs. *Inv/SmoM2/Survivin* GOF), and (f) the genes upregulated upon *Survivin* deletion in SCs (up *SmoM2/Survivin cKO* vs. *Krt14/SmoM2*). We found 241 genes commonly

upregulated in the abovementioned signatures involved in epidermal differentiation (e.g., Krt2 and Nrp1), lipid metabolism and lipid synthesis (e.g., Elovl3, Elovl6, Fa2H, Lpl, Lss, Mgll, and Scd1) associated with keratinocyte and skin barrier function (Fig. 6D-F; ref. 21).

Altogether our results identified the genes modulated by *Survivin* expression in the context of *SmoM2*-expressing cells that may promote oncogene-targeted cell proliferation and survival and prevent their terminal differentiation.

RESEARCH ARTICLE Canato et al.

Sgk1 Is a Survivin-Regulated Gene Essential for BCC Formation

As Survivin expression is essential for BCC formation, we assessed whether, among the genes regulated by SmoM2 in a Survivin-dependent manner, there are genes that promote BCC formation and could be targeted pharmacologically, as an alternative to the use of Survivin inhibitor. Among the 82 genes that were commonly upregulated by Survivin expression across all three experimental conditions tested, Sgk1 seems to be a potential candidate gene regulating Survivin-mediated stemness during BCC formation (Fig. 6A-C). SGK1 shares structural and functional similarities with the AKT family of kinases, is expressed in several cancer types, and has been involved in cancer cell proliferation, apoptosis, and migration (20). IHC showed that SGK1 is not expressed in hyperplasia, starts to be expressed in dysplasia, and persists at the BCC stage in Krt14/SmoM2 and Inv/SmoM2/Survivin GOF mice, but not in preneoplastic lesions from Inv/SmoM2 mice (Fig.6G; Supplementary Fig. S8A).

To assess the role of SGK1 in regulating BCC formation, we treated *Krt14/SmoM2* and *INV/SmoM2/Survivin GOF* mice 8 weeks after tamoxifen administration with SGK1 inhibitor (SGK1 Inh, SI113; ref. 22) for 4 weeks (Fig. 7A). Interestingly, SGK1 inhibitor treatment led to a decrease in the density of *SmoM2*-expressing lesions and a decrease in the number of dysplastic lesions that progressed into BCC, resulting in a 10- and 27-fold decrease in tumor burden in the *Krt14/SmoM2* and *Inv/SmoM2/Survivin GOF* mice, respectively, compared with the control group (Fig. 7B–D; Supplementary Fig. S8B and S8C).

We next assessed the mechanism by which SGK1 inhibitor prevents BCC formation. As SGK1 has been described to regulate apoptosis and proliferation, we performed immunostaining for the apoptotic marker (CC3) and assessed proliferation using Ki67 expression in Krt14/SmoM2 and Inv/ SmoM2/Survivin GOF mice. SGK1 inhibition led to an increase in the number of apoptotic cells per lesion from 1.6% to 6.2% in Krt14/SmoM2 and from 3.5% to 12% in Inv/SmoM2/ Survivin GOF after SGK1 inhibitor administration (Fig. 7E-G). In addition, the number of proliferative Ki67+ cells was decreased from 20.9% to 9.2% in Krt14/SmoM2 and from 18.3% to 13.3% in Inv/SmoM2/Survivin GOF after SGK1 inhibition (Fig. 7H and I). Moreover, SGK1 inhibition promoted differentiation of the basal cells in tumorigenic lesions as indicated by an increase in KRT10 expression in basal compartment (KRT14-expressing cells; Fig. 7J and K; Supplementary Fig. S8D). To uncover whether SGK1 inhibition affects Survivin expression, we assessed Survivin expression in lesions from *Krt14/SmoM2* mice treated with SGK1 inhibitor and controls. We found that SGK1 inhibition led to a decrease in the proportion of tumorigenic cells expressing Survivin, suggesting that SGK1 can promote Survivin expression (Supplementary Fig. S8E and S8F).

Altogether, these experiments demonstrate that SGK1 inhibition prevents BCC formation by decreasing cell proliferation while promoting apoptosis and differentiation, phenocopying the effect of *Survivin* deletion or pharmacologic inhibition and demonstrating that pharmacologic SGK1 inhibition represents an alternative strategy to prevent BCC formation.

DISCUSSION

In this study, we define the mechanisms underlying the relative competence of SCs and Ps to mediate BCC initiation and identify *Survivin* as a key factor that confers SCs competence to initiate BCC formation.

Transcriptional profiling of SCs and Ps identify Survivin as being strongly upregulated in SCs compared with Ps in the mouse epidermis upon Hh signaling pathway activation. The loss of function of Survivin in SCs in the presence or absence of oncogene expression leads to a rapid disappearance of normal SCs and oncogene-targeted SCs and decreases their ability to initiate BCC. Conversely, Survivin overexpression in Ps decreases their rapid clonal loss and promotes their ability to initiate BCC formation after SmoM2 expression. Interestingly, Survivin was also identified as upregulated in human keratinocyte SCs that give rise in vitro to colonies that are more proliferative and clonogenic called holoclones, compared with colonies composed of committed progenitors that are non-clonogenic referred to as meroclones and paraclones (23), suggesting that Survivin expression might be a hallmark of epidermal SCs across species.

Single-cell analysis combined with immunostaining and functional experiments reveal that *Survivin* expression increases cell proliferation, stimulates self-renewing divisions, and restricts apoptosis and terminal differentiation of oncogenetargeted cells, promoting clonal persistence, clonal expansion, and tumor initiation (Supplementary Fig. S9).

The role of Survivin in tumor progression has been described in many tumor types, wherein its expression has been correlated with enhanced cell proliferation and survival. For this reason, several Survivin inhibitors have been developed and are currently tested in clinical trials (14). The role of Survivin in tumor progression has been reported in Sonic Hedgehog (SHH) medulloblastoma, a pediatric brain tumor that arises upon constitutive activation of the Hh signaling pathway during cerebellar development. That study reported that in established SHH medulloblastoma, Survivin deletion or inhibition led to medulloblastoma shrinkage in a grafting heterotopic model (24). Although the role of Survivin in tumor progression has been previously described, our study now shows that Survivin expression is essential at the earliest stage of tumor initiation and that confers to SCs the relative competence of tumor formation. Our data also indicate that Survivin overexpression confers stemness to more committed cells and overcomes their inability to mediate BCC formation. Survivin overexpression acts in the epidermis similarly as inflammation promotes tumorigenesis in the intestine, inducing dedifferentiation of non-SCs and promoting their ability to acquire tumor-initiating capacity (25). Our data also show that short-term administration of Survivin inhibitor leads to shrinkage and elimination of preneoplastic lesions and prevents BCC progression.

Finally, we have identified SGK1 inhibition as a new strategy to block the promotion of cell survival and cell proliferation mediated by *SmoM2* in a *Survivin*-dependent manner and to prevent BCC initiation. Several SGK1 inhibitors have recently been developed and described to lead to tumor shrinkage alone or in combination with other treatment options in a variety of tumor types (20). Our data show that SGK1 inhibition

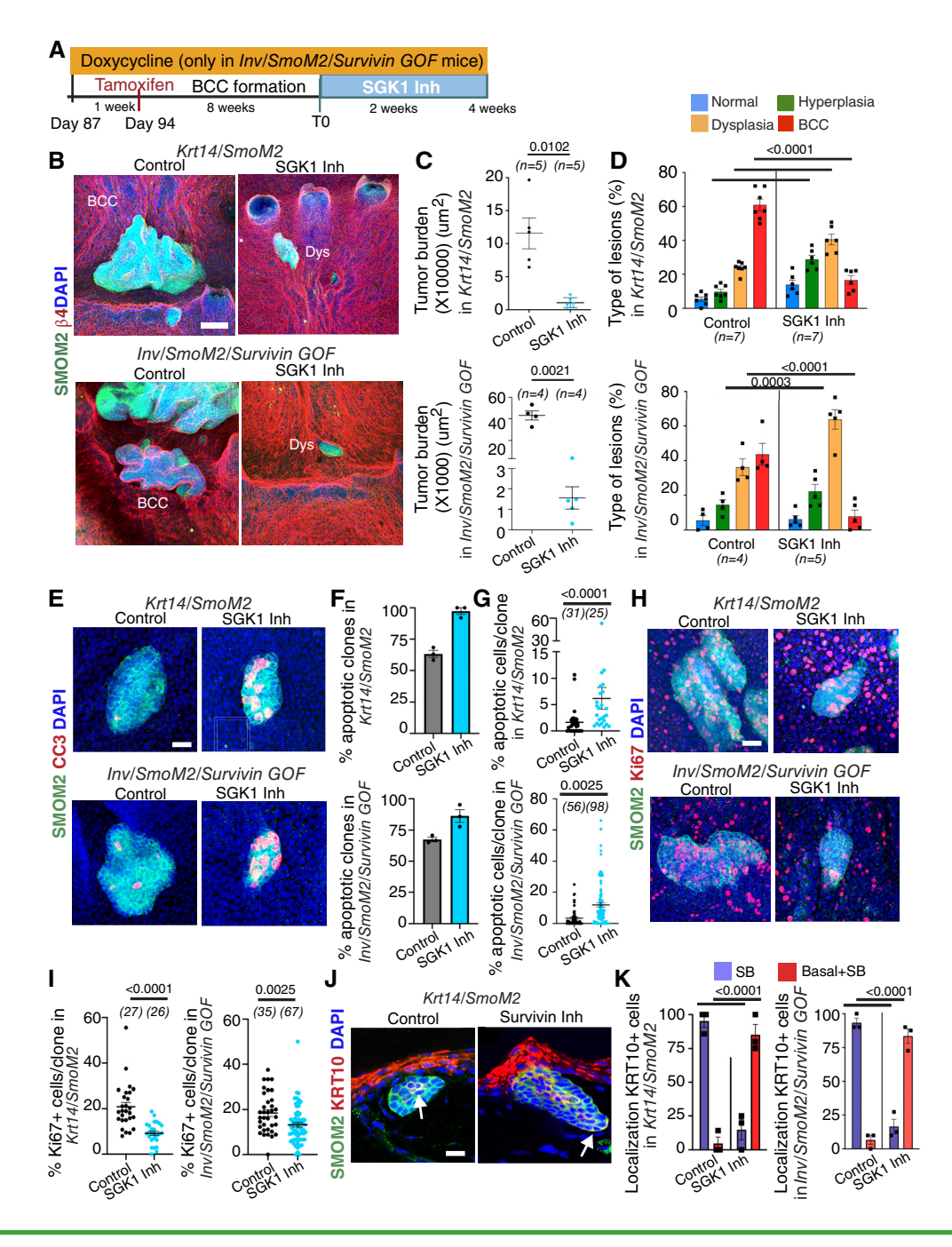


Figure 7. SGK1 inhibition prevents BCC formation in Survivin-expressing cells. A, Protocol used for the treatment of Krt14/SmoM2 and Inv/SmoM2/ Survivin GOF mice with SGK1 inhibitor. B, Confocal analysis of immunostaining for SmoM2 and \(\beta 4-integrin on whole mounts of tail skin of \(Krt14/SmoM2 \) and Inv/SmoM2/Survivin GOF mice treated 4 weeks with SGK1 inhibitor and control mice. C, Tumor burden in Krt14/SmoM2 and Inv/SmoM2/SurvivinGOF mice treated for 4 weeks with SGK1 inhibitor and control mice (n = mice). Statistical significance was assessed using the Welch t test. **D**, Quantification of the types of lesions in Krt14/SmoM2 and Inv/SmoM2/Survivin GOF mice treated for 4 weeks with SGK1 inhibitor and control mice (n = mice). Statistical significance was assessed using two-way ANOVA with the Šidák multiple comparison test. E, Immunostaining for CC3 and SmoM2 after SGK1 inhibitor treatment in Krt14/SmoM2 and Inv/SmoM2/Survivin GOF mice. F, Quantification of the number of apoptotic clones at 2 weeks of SGK1 inhibitor treatment in Krt14/SmoM2 and Inv/SmoM2/Survivin GOF mice (n = 3 mice/group). Significance was determined using the Welch t test. G , Quantificationof the number of apoptotic cells per clone at 2 weeks of SGK1 inhibitor treatment in Krt14/SmoM2 and Inv/SmoM2/Survivin GOF mice (n = clones from three and two mice: Krt14/SmoM2 and Inv/SmoM2/Survivin GOF mice, respectively). Statistical significance was assessed using the Mann-Whitney test. H, Confocal analysis of immunostaining for SmoM2 and Ki67 on whole mounts of tail skin of Krt14/SmoM2 and Inv/SmoM2/Survivin GOF mice at 2 weeks of the SGK1 inhibitor treatment. I, Percentage of Ki67+ cells per clone at 2 weeks of Survivin inhibitor treatment in Krt14/SmoM2 and Inv/SmoM2, Survivin GOF mice (n = clones from three mice). Significance was determined using the Mann-Whitney test. **J,** Immunostaining for SmoM2 and KRT10 in sections in Krt14/SmoM2 lesions at 2 weeks of SGK1 inhibitor treatment. K, Quantification of tumorigenic lesions from Krt14/SmoM2 and Inv/SmoM2/SmoM2Survivin GOF mice containing KRT10 in suprabasal (SB) or basal + SB layers at 2 weeks of SGK1 inhibitor treatment (n = 3 mice/group). Statistical analysis was determined using two-way ANOVA. Error bars represent the mean ± SEM in each figure. Scale bar, 50 µm in B and 20 µm in E, H, and J. Number of clones counted presented in parentheses.

RESEARCH ARTICLE Canato et al.

can prevent the conversion of preneoplastic lesions into invasive tumors, representing an alternative to the use of Survivin inhibitors in the prevention of BCC progression.

METHODS

Mice

Krt14-CreER (RRID: IMSR_JAX:005107; ref. 26) transgenic mice were kindly provided by E. Fuchs, The Rockefeller University. Inv-CreER mice were generated in Cédric Blanpain laboratory (RRID: IMSR_JAX:019380; ref. 6). Ptch1^{fl/fl}, Rosa-YFP, and Rosa-SmoM2-YFP mice were obtained from the JAX repository (RRID: IMSR_JAX:012457, IMSR_JAX:006148, and IMSR_JAX:005130, respectively). K14-rtTA transgenic mice (27) were provided by E. Fuchs (RRID: IMSR_JAX:008099). The Survivin^{fl/fl} animals were kindly provided by E.M. Conway.

Mouse colonies were maintained in a certified animal facility in accordance with the European guidelines for the laboratory animal use and care based on the 2010/63/EU Directive. Experiments involving mice presented in this work were approved by the Animal Welfare and Ethics Body, Direção-Geral da Alimentação e Veterinária (Portuguese Authority) under protocol number 011681 and Comité d'Ethique du Bien Être Animal (ULB) under protocol number 483N.

Skin Tumor Induction

For tumor induction, 1.5-month-old mice were used. Krt14/ SmoM2, SmoM2/Survivin cKO, Krt14/Ptch1 cKO, and Krt14/Ptch1 cKO/ Survivin cKO mice received an intraperitoneal injection of 0.1 mg (0.5 mg/mL) of tamoxifen (ref. T5648-0005, Sigma-Aldrich). Inv/ SmoM2, Inv/SmoM2/Survivin GOF, Inv/Ptch1 cKO, and Inv/Ptch1 cKO/ Survivin GOF mice received one intraperitoneal injection of 2.5 mg (12.5 mg/mL) of tamoxifen to achieve similar levels of recombination in the different models. Inv/SmoM2/Survivin GOF and Inv/Ptch1 cKO/ Survivin GOF mice received an intraperitoneal injection (2 mg/mL in PBS) weekly followed by doxycycline in drinking water (2 mg/mL $\,$ daily) until the animal was euthanized. Mice were sacrificed and analyzed at different time points after tamoxifen administration. SmoM2 animals were heterozygous for the SmoM2 mutation in the Rosa locus. Ptch1cKO were Ptch1fl/fl, homozygous for the floxed allele. Animals showing low or patchy mCherry expression were excluded from this study

The tail skin and ventral skin were used in our analysis. Specifically, in the SmoM2 model, the tail skin was analyzed, as in this model, BCC arises in the tail, paws, and ear (6).

The ventral skin was the one used in the analysis of the *Ptch1 cKO* model, as tumors in this model arise in the ventral and back skin and ears (5).

Lineage-Tracing Experiments during Skin Homeostasis

For the lineage-tracing experiments, 1.5-month-old mice were used. *Krt14/YFP* mice received an intraperitoneal injection of 0.1 mg (0.5 mg/mL) of tamoxifen (ref. T5648-0005, Sigma-Aldrich) and *Inv-CreER/Rosa-YFP* received one intraperitoneal injection of 2.5 mg (12.5 mg/mL) of tamoxifen to achieve similar levels of recombination in the different models. *Inv/YFP/Survivin GOF* mice first received an intraperitoneal injection followed by the administration of 2 mg/mL of doxycycline in drinking water until the animals were euthanized (every week), and 1 week after the first injection of doxycycline, they received an intraperitoneal injection of 2.5 mg (12.5 mg/mL) of tamoxifen. Mice were sacrificed and analyzed at different time points after tamoxifen administration. All mice were heterozygous for *Rosa-YFP*. Animals showing low or patchy mCherry expression were excluded from this study.

SGK1 Inhibitor Administration

SGK1 inhibitor (SI113) was kindly provided by Silvia Schenone and Giancarlo Grossi (University of Genoa). During SGK1 inhibitor treatment, mice received SGK1 inhibitor at a concentration of 50 mmol/L two times per day by intraperitoneal injection for 4 weeks. The SGK1 inhibitor was dissolved in 0.9% NaCl solution.

Survivin Inhibitor Administration

During Survivin inhibitor treatment, mice received 5 mg/kg/day of YM155 (Selleckchem, #S1130) by continuous subcutaneous infusion using micro-osmotic pump (model 1002, ALZET). Survivin inhibitor was dissolved in 1× PBS solution.

Whole Mounts of Tail Epidermis

Whole mounts of tail epidermis were performed as previously described (2).

Specifically, pieces of tail were incubated for 1 hour at 37°C in 20 mmol/L EDTA in PBS in a rocking plate, then using forceps, the dermis and epidermis were separated, and the epidermis was fixed for 30 minutes in 4% paraformaldehyde (PFA) in agitation at room temperature and washed three times with PBS.

For immunostaining, tail skin pieces were blocked with blocking buffer for 3 hours (PBS, 5% horse serum, and 0.8% Triton) in a rocking plate at room temperature. Then, the skin pieces were incubated with primary antibodies diluted in blocking buffer overnight at 4°C; the next day, they were washed with 0.2% PBS-Tween for 3×10 minutes at room temperature, and then incubated with secondary antibodies diluted in blocking buffer for 3 hours at room temperature, washed 2×10 minutes with 0.2% PBS-Tween, and washed for 10 minutes in PBS. Finally, they were incubated in Hoechst (1:1,000) diluted in PBS for 30 minutes at room temperature in the rocking plate, washed 3×10 minutes in PBS, and mounted in Dako mounting medium supplemented with 2.5% DABCO (Sigma). The primary antibodies used were goat anti-GFP (1:800, ref. ab6673, Abcam, RRID: AB_300798), rat anti- β 4-integrin (1:500, ref. 553745, BD Pharmingen, RRID: AB_395027), rabbit anti-cleaved-caspase-3 (1:600, ref. AF835, R&D Systems, RRID: AB_2243952), rabbit anti-Ki67 (1:1000, ab15580, Abcam, RRID: AB_443209), and rabbit anti-SURVIVIN (1:800, ref. 2808, Cell Signaling Technology, RRID: AB_2063948). Secondary antibodies (R&D Systems) used were anti-goat, anti-rat, and antirabbit conjugated to Alexa Fluor 488 (goat, ref. A-11055, Invitrogen, RRID: AB_2534102), to Rhodamine Red-X (rat, ref. 712-295-153, Jackson ImmunoResearch, RRID: AB_2340676; rabbit, 711-295-152, Jackson ImmunoResearch, RRID: AB_2340613), and to Alexa Fluor 647 (rat, ref. 712-605-153, Jackson ImmunoResearch, RRID: AB_2340694; rabbit, 711-605-152, Jackson ImmunoResearch, RRID: AB_2492288). Images were acquired using Z-stacks with an inverted confocal microscope LSM 980 (Carl Zeiss).

Immunostaining in Sections

The tail in the SmoM2 model and ventral skin in the *Ptch1cKO* model were embedded in optimal cutting temperature compound (Sakura, ref. 4583) and cut into 7- to 8-µm frozen sections using Leica CM3050S cryostat (Leica Microsystems). Frozen sections were dried and fixed with 4% PFA for 10 minutes at room temperature and blocked with a blocking buffer (1× PBS, 5% horse serum, 1% BSA, and 0.2% Triton) for 1 hour. Skin sections were incubated with primary antibodies overnight at 4°C, washed with 1× PBS for 3 × 5 minutes, and then incubated with secondary antibodies and Hoechst (1:1,000, ref. H3570, Invitrogen) for 1 hour at room temperature in agitation. Finally, sections were washed with 1× PBS for 3×5 minutes at room temperature and mounted in DAKO mounting media (ref. 237-C056330-2, Dako). Primary and secondary antibodies used were diluted in blocking buffer. The primary antibodies used

were goat anti-GFP (1:500, ref. ab6673, Abcam, RRID: AB_300798), rat anti-β4-integrin (1:500, ref. 553745, BD Pharmingen, RRID: AB_395027), rabbit anti-cleaved-caspase-3 (1:600, ref. AF835, R&D Systems, RRID: AB_2243952), rabbit anti-KRT10 (1:4,000, PRB-159P, Covance/IMTEC, RRID: AB_291580), rabbit anti-AURKB (1:200, ab2254, Abcam, RRID: AB_302923), and chicken anti-GFP (1:400, ab13970, Abcam, RRID: AB_300798). The secondary antibodies used were anti-goat, anti-rat, anti-rabbit, and anti-chicken conjugated to Alexa Fluor 488 (goat, ref. A-11055, Invitrogen, RRID: AB_2534102), to Rhodamine Red-X (rat, ref. 712-295-153, Jackson ImmunoResearch, RRID: AB_2340676; rabbit, 711-295-152, Jackson ImmunoResearch, RRID: AB_2340613), and to Alexa Fluor 647 (rat, ref. 712-605-153, Jackson ImmunoResearch, RRID: AB_2340694; rabbit, 711-605-152, Jackson ImmunoResearch, RRID: AB_2492288). Images were acquired using inverted confocal microscope LSM 980 (Carl Zeiss).

BrdU Proliferation Experiments

For proliferation assay, mice received intraperitoneal injection of 3 mg/mL BrdU (ref. B9285, Merck). Mice were sacrificed after 3 days and whole-mount staining for the tail was performed. Pieces of tail were first stained for anti-GFP (1:800, ref. ab6673, Abcam, RRID: AB_300798), and then, skin pieces were washed 3 × 10 minutes with a washing buffer (1× PBS and 0.2% Tween) and fixed for 15 minutes in 4% PFA. Skin pieces were then washed 3 × 10 minutes and incubated for 20 minutes with 1 mol/L HCL at 37°C. Skin pieces were incubated with Alexa Fluor 647 mouse anti-BrdU (1:200, ref. 560209, BD Pharmingen, RRID: AB_1645615) overnight at room temperature under agitation. Finally, the skin pieces were washed 3 × 10 minutes with 1× PBS, incubated with Hoechst (1:1,000) and washed 3 × 10 minutes with 1× PBS and mounted in DAKO mounting media. Images were acquired using Z-stacks using an inverted confocal microscope LSM 980 (Carl Zeiss).

IHC

For SGK1 IHC, 5-µm paraffin sections were deparaffinized, rehydrated, followed by antigen unmasking performed for 20 minutes in sodium citrate (pH 6). Rabbit anti-SGK1 antibody (1:100, ref. PAS-87746, Invitrogen, RRID: AB_2804383) was used.

ISH/RNA FISH

For ISH of *Birc5* and *Defb6*, 5-µm PFA-fixed paraffin sections were deparaffinized and the *in situ* protocol was performed according to the manufacturer's instructions (Advanced Cell Diagnostics). The following mouse probes were used: Mm-Birc5 (422701) and Mm-Defb6 (430141). ISH was performed according to the manufacturer's instructions (RNAscope Multiplex Fluorescent V2 Assay, ACDBio). In IF staining for GFP+ and *Defb6* ISH in the same section, we first performed ISH for *Defb6* on section and then regular IF staining for GFP, which included steps of blocking the tissue for 1 hour at room temperature and overnight antibody incubation at 4°C, then followed by secondary antibody for 1 hour to detect the signal of GFP.

Analysis of Clone Survival, Size, and Apoptosis

Quantification of the proportion of surviving clones (persistence) and the basal clone size were determined by counting the number of SmoM2-positive cells in each clone using orthogonal views of the whole mount of tail epidermis in the interscale region of IFE as described previously (1, 2). The number of active-caspase-3, Ki67, and SURVIVIN cells and positive-BrdU-doublet cells in each clone were also quantified using orthogonal views of the whole mount of tail epidermis. $\beta 4\text{-integrin}$ staining was used to classify the clone according to their location in basal or suprabasal layers.

FACS Isolation of Tumors and Bulk RNA-seq

Tail skins were separated from the tail bone and incubated overnight in trypsin at 4°C (Gibco). The next day, the epidermis was separated from the dermis and incubated for 20 minutes in trypsin on a rocking plate. Trypsin was neutralized by adding DMEM containing 10% Chelex FBS. Epidermal solution was collected and resuspended in a blocking buffer (1× DPBS, 5 mmol/L EDTA, and 5% chelated FBS) and filtered with a 70-µm strainer, then by a 40-µm strainer. The obtained single-cell solution was then centrifuged at 500g for 10 minutes at 4°C, and the pellet was resuspended in FACS buffer (1× DPBS, 2 mmol/L EDTA, and 2% chelated FBS). Cells were stained using rat Biotin anti-CD34 (1:50, ref. 13-0341-85, eBioscience, RRID: AB_466426) and rat anti-α6-integrin-PE (1:600, ref. 12-0495-83, eBioscience, RRID: AB_891474) followed by the secondary antibody APC-streptavidin (1:400, ref. 554067, BD Pharmingen, RRID: AB_10050396), and Hoechst 33342 (1:4,000, Thermo Fisher Scientific, ref. H3570, 10 mg/mL). Cells were sorted at the Flow Cytometry Platform (Champalimaud Foundation and ULB) using BD FACSAria Fusion Cell Sorter with a 85-µm nozzle and 2.0-µm filter. Forward versus side scatter gating was used to identify the cells of interest based on size and granularity.

RNA Extraction, RT-PCR, and qRT-PCR

RNA extraction was performed using Rneasy micro kit (ref. 74004, QIAGEN) according to the manufacturer's instructions. cDNA was synthesized using high-capacity RNA-to-cDNA kit (ref. 4387406, Thermo Fisher Scientific) according to the manufacturer's instructions. qRT-PCR amplifications were performed in a QuantStudio 5 Real-Time PCR machine (Bio-Rad) using a 384-well plate with NZYSupreme qPCR Green Master Mix (ref. MB41903, NZYtech) and a set of primers (mouse BIRC5, F:5'-CACCTTCAAGAACTGGCCCTT-3', R:5'-TTCCCAGCCTTCC AATTCCTTA-3'; mouse HPRT, F:5'-GCAGTACAGCCCCAAAAT GG-3', R:5'-TCCAACAAAGTCTGGCCTGT-3') according to the manufacturer's instructions. The fold difference in gene expression was calculated by the relative quantification method using the mathematical equation 2-ΔΔCT.

Bulk RNA-seq

About 10.000 to 200.000 FACS cells were collected directly in the lysis buffer provided by the manufacturer (RNeasy Micro kit, QIAGEN), and RNA extraction was then carried out according to the manufacturer's protocol. Indexed cDNA libraries were obtained using the Ovation SoLo RNA-seq Systems (NUGEN) following the manufacturer's recommendations. The multiplexed libraries were loaded on flow cells and sequences were produced using a NovaSeq 6000 S2 Reagent Kit (200 cycles from NovaSeq 6000 System, Illumina) on a NovaSeq 6000 System (Illumina).

Reads were mapped against the mouse reference genome (GRCm38/mm10) using STAR software (RRID: SCR_004463; ref. 28) to generate read alignments for each sample. Annotations for the reference genome (Mus_musculus.GRCm38.87.gtf) were obtained from ftp.ensembl.org. After transcripts assembling, gene level counts were obtained using htseq-count (RRID: SCR_011867; ref. 29) and normalized to 20 million alignment reads. Genes with individual sample expression levels lower than 10 and replicate average expression levels lower than 20 were filtered out. The fold changes of average gene expression for the replicates were used to calculate the level of differential gene expression between different cell populations. Genes with an expression fold change greater or equal to 2 were considered upregulated and those with an expression fold change lower or equal to 0.5 were considered downregulated.

RESEARCH ARTICLE Canato et al.

scRNA-seq

We sorted cells for $\alpha6^{\text{high}}/\text{CD34}^-/\text{YFP}^+$ from Inv/SmoM2 (n=8,046) and Inv/SmoM2/Survivin GOF mice. A total of 10,000 cells were loaded onto each channel of the Chromium Single Cell 3' microfluidic chips (V2-chemistry, PN-120232, 10X Genomics) and barcoded with a 10× Chromium Controller according to the manufacturer's recommendations (10X Genomics). RNA from the barcoded cells was subsequently reverse-transcribed, followed by amplification, shearing 5' adapter, and sample index attachment. The libraries were prepared using the Chromium Single Cell 3' Library Kit (V3-chemistry, PN-120233, 10X Genomics) and sequenced on an Illumina NovaSeq 6000 (paired-end 100-bp reads).

Single-Cell Transcriptomic Data Analysis

Sequencing reads were aligned and annotated with the mm10-2020-A reference dataset as provided by 10X Genomics and demultiplexed using Cell Ranger (v.6.1.1; RRID: SCR_023221; ref. 30) with default parameters. Further downstream analyses were carried out individually for each of the two samples (Inv/SmoM2 and Inv/SmoM2/Survivin GOF).

Quality control and downstream analysis were performed using the Seurat R package (RRID: SCR_016341; v4.2.0; ref. 31). For each sample, all of the cells passed the following criteria: showed expression of more than 2,000 and less than 6,000 unique genes and had less than 10% unique molecular identifier (UMI) counts belonging to mitochondrial sequences. Read counts were normalized by NormalizeData() function of Seurat, with the parameter "normalization.method = "LogNormalize" and scale.factor = 10,000." A prinicipal component analysis (PCA) for each sample was calculated using the scaled expression data of the most variable genes (identified as outliers on a mean/variability plot, implemented in the FindVariableGenes()). Uniform Manifold Approximation and Projection (UMAP) calculation (32) and graph-based clustering were done for each sample using the appropriate functions from Seurat (default parameters) with the respective 30 PCA results as input.

The clusters expressing immune cell (*Cd74* and *Cd52*) and fibroblast (*Vim*) markers were excluded, and dimensionality was recalculated. The final resolutions were set to 0.5 after testing a range from 0.2 to 0.7. Given that the obtained clustering sensitivity for a given resolution is dependent on the number of cells of that subpopulation in each respective sample, we swept over the same range of resolutions for the other samples, to assure the presence/absence of described clusters in all samples. Selected resolutions are the best to reflect the biological heterogeneity between different cell types. A Wilcoxon rank-sum test was used to define marker genes for each cluster using the *FindAllMarkers()* function. Benjamini–Hochberg FDR correction for potential cluster marker genes across all samples using the p.adjust method in *R* and only markers expressed in at least 25% of the cells of the cluster, having an average log₂ fold change of at least 0.25 were reported.

For visualization and comparison between different samples, we integrated Inv/SmoM2 and Inv/SmoM2/Survivin GOF using the Seurat package's standard canonical correlation analysis and multiple nearest neighbors (CCA-MNN)-based data integration workflow. Feature selection was performed using the FindVariableFeatures function from Seurat with default parameters, selecting the 2,000 most variable genes. CCA followed by integration anchors selection was then performed on the selected features using the FindIntegrationAnchors() function from Seurat, taking the first 30 dimensions from the CCA into account, as described on the standard workflow of Seurat (RRID: SCR_ 016341). These anchors were then used to integrate the data using the IntegrateData() function. Following the annotation of clusters, clusters sharing the same cell identities were merged into a single cluster. This merging process was performed after confirming that there were no differences in terms of gene expression between these clusters with the same cell identity. The assessment of gene expression was based on both well-known marker genes and marker genes determined using the Wilcoxon rank-sum test.

On the individual and integrated datasets, to identify cell proliferation stages, the S-phase and G_2 -M-phase scores were computed by *CellCycleScoring()* function, implemented in Seurat.

Statistical Analysis

All statistical analyses were performed using GraphPad Prism v.8.0.1 (www.graphpad.com; RRID: SCR_002798) software. Data are expressed as mean \pm SEM. Normality was tested using Shapiro–Wilk test. For the database that followed normality, P values were estimated with unpaired t test for two experimental groups or for multiple comparison two-way ANOVA. For the dataset that did not follow the normal distribution, P values were calculated using the Mann–Whitney test. For all the figures, the number of mice and number of clones is indicated in the figure body or figure legend.

The sample size was chosen based on previous experience in the laboratory for each experiment to yield high power to detect specific effects. No statistical methods were used to predetermine sample size.

Investigators were not blinded to mouse genotypes during experiments. Researchers were not blinded when performing imaging and quantification.

Data Availability

Data associated with this study have been deposited in the NCBI Gene Expression Omnibus under accession numbers GSE277554 (bulk RNA-seq) and GSE277555 (scRNA-seq).

Authors' Disclosures

No disclosures were reported.

Authors' Contributions

S. Canato: Formal analysis, investigation, methodology. R. Sarate: Formal analysis, investigation. S. Carvalho-Marques: Formal analysis, investigation, methodology. R. Maia Soares: Investigation, methodology. Y. Song: Data curation, formal analysis. S. Monteiro-Ferreira: Investigation. P. Vieugué: Investigation. M. Liagre: Investigation. G. Grossi: Resources. E. Cardoso: Investigation. C. Dubois: Investigation. E.M. Conway: Resources. S. Schenone: Resources. A. Sánchez-Danés: Conceptualization, resources, supervision, funding acquisition, investigation, writing-original draft. C. Blanpain: Conceptualization, resources, supervision, funding acquisition, writing-original draft.

Acknowledgments

We thank the Champalimaud and ULB animal facility, ULB genomic core facility (F. Libert and A. Lefort), and Champalimaud ABBE platform and ULB LiMiF (J.M. Vanderwinden), for help with microscopy. A. Sánchez-Danés, S. Canato, and R. Maia Soares were supported by QuantOCancer Project Horizon European Union's Horizon 2020 program (grant agreement No 810653). S. Carvalho-Marques is supported by Fundação para a Ciência e Tecnologia (2021.05801.BD). This project is supported by a Fundação para a Ciência e Tecnologia grant to A. Sánchez-Danés (PTDC/MED-ONC/5553/2020). R. Sarate and M. Liagre are supported by Télévie. C. Blanpain is supported by the WEL Research Institute, FNRS, Télévie, Fond Erasme, Fondation contre le Cancer, ULB Foundation, and European Research Council.

Note

Supplementary data for this article are available at Cancer Discovery Online (http://cancerdiscovery.aacrjournals.org/).

Received February 22, 2024; revised September 11, 2024; accepted November 7, 2024; published first November 11, 2024.

REFERENCES

- Mascré G, Dekoninck S, Drogat B, Youssef KK, Broheé S, Sotiropoulou PA, et al. Distinct contribution of stem and progenitor cells to epidermal maintenance. Nature 2012;489:257–62.
- Sánchez-Danés A, Hannezo E, Larsimont JC, Liagre M, Youssef KK, Simons BD, et al. Defining the clonal dynamics leading to mouse skin tumour initiation. Nature 2016;536:298–303.
- Blanpain C, Simons BD. Unravelling stem cell dynamics by lineage tracing. Nat Rev Mol Cell Biol 2013;14:489–502.
- Epstein EH. Basal cell carcinomas: attack of the hedgehog. Nat Rev Cancer 2008:8:743–54.
- Youssef KK, Lapouge G, Bouvrée K, Rorive S, Brohée S, Appelstein O, et al. Adult interfollicular tumour-initiating cells are reprogrammed into an embryonic hair follicle progenitor-like fate during basal cell carcinoma initiation. Nat Cell Biol 2012;14:1282–94.
- Youssef KK, Van Keymeulen A, Lapouge G, Beck B, Michaux C, Achouri Y, et al. Identification of the cell lineage at the origin of basal cell carcinoma. Nat Cell Biol 2010;12:299–305.
- Dlugosz A. The hedgehog and the hair follicle: a growing relationship. J Clin Invest 1999;104:851–3.
- Larsimont JC, Youssef KK, Sánchez-Danés A, Sukumaran V, Defrance M, Delatte B, et al. Sox9 controls self-renewal of oncogene targeted cells and links tumor initiation and invasion. Cell Stem Cell 2015;17: 60–73.
- Chen T, Heller E, Beronja S, Oshimori N, Stokes N, Fuchs E. An RNA interference screen uncovers a new molecule in stem cell self-renewal and long-term regeneration. Nature 2012;485:104–8.
- Hegde GV, de la Cruz C, Giltnane JM, Crocker L, Venkatanarayan A, Schaefer G, et al. NRG1 is a critical regulator of differentiation in TP63-driven squamous cell carcinoma. Elife 2019;8:e46551.
- Vassar R, Fuchs E. Transgenic mice provide new insights into the role of TGF-alpha during epidermal development and differentiation. Genes Dev 1991;5:714–27.
- Leigh IM, Navsaria H, Purkis PE, McKay IA, Bowden PE, Riddle PN. Keratins (K16 and K17) as markers of keratinocyte hyperproliferation in psoriasis in vivo and in vitro. Br J Dermatol 1995;133: 501, 11
- 13. Hess J, Angel P, Schorpp-Kistner M. AP-1 subunits: quarrel and harmony among siblings. J Cell Sci 2004;117:5965-73.
- Altieri DC. Survivin, cancer networks and pathway-directed drug discovery. Nat Rev Cancer 2008;8:61–70.
- Murata-Hori M, Tatsuka M, Wang YL. Probing the dynamics and functions of aurora B kinase in living cells during mitosis and cytokinesis. Mol Biol Cell 2002:13:1099–108.
- Dekoninck S, Hannezo E, Sifrim A, Miroshnikova YA, Aragona M, Malfait M, et al. Defining the design principles of skin epidermis postnatal growth. Cell 2020;181:604–20.e22.

- 17. Joost S, Zeisel A, Jacob T, Sun X, La Manno G, Lönnerberg P, et al. Single-cell transcriptomics reveals that differentiation and spatial signatures shape epidermal and hair follicle heterogeneity. Cell Syst 2016;3:221–37.e9.
- Joost S, Jacob T, Sun X, Annusver K, La Manno G, Sur I, et al. Single-cell transcriptomics of traced epidermal and hair follicle stem cells reveals rapid adaptations during wound healing. Cell Rep 2018;25:585–97.e7.
- Bansaccal N, Vieugue P, Sarate R, Song Y, Minguijon E, Miroshnikova YA, et al. The extracellular matrix dictates regional competence for tumour initiation. Nature 2023;623:828–35.
- Sang Y, Kong P, Zhang S, Zhang L, Cao Y, Duan X, et al. SGK1 in human cancer: emerging roles and mechanisms. Front Oncol 2020; 10:608722.
- Vietri Rudan M, Watt FM. Mammalian epidermis: a compendium of lipid functionality. Front Physiol 2021;12:804824.
- Talarico C, D'Antona L, Scumaci D, Barone A, Gigliotti F, Fiumara CV, et al. Preclinical model in HCC: the SGK1 kinase inhibitor SI113 blocks tumor progression in vitro and in vivo and synergizes with radiotherapy. Oncotarget 2015;6:37511–25.
- 23. Enzo E, Secone Seconetti A, Forcato M, Tenedini E, Polito MP, Sala I, et al. Single-keratinocyte transcriptomic analyses identify different clonal types and proliferative potential mediated by FOXM1 in human epidermal stem cells. Nat Commun 2021;12:2505.
- Brun SN, Markant SL, Esparza LA, Garcia G, Terry D, Huang JM, et al. Survivin as a therapeutic target in sonic hedgehog-driven medulloblastoma. Oncogene 2015;34:3770-9.
- Schwitalla S, Fingerle AA, Cammareri P, Nebelsiek T, Göktuna SI, Ziegler PK, et al. Intestinal tumorigenesis initiated by dedifferentiation and acquisition of stem-cell-like properties. Cell 2013;152:25–38.
- Vasioukhin V, Degenstein L, Wise B, Fuchs E. The magical touch: genome targeting in epidermal stem cells induced by tamoxifen application to mouse skin. Proc Natl Acad Sci U S A 1999;96:8551–6.
- 27. Nguyen H, Rendl M, Fuchs E. Tcf3 governs stem cell features and represses cell fate determination in skin. Cell 2006;127:171-83.
- Dobin A, Davis CA, Schlesinger F, Drenkow J, Zaleski C, Jha S, et al. STAR: ultrafast universal RNA-seq aligner. Bioinformatics 2013;29: 15–21.
- Anders S, Pyl PT, Huber W. HTSeq-a Python framework to work with high-throughput sequencing data. Bioinformatics 2015;31:166–9.
- Zheng GX, Terry JM, Belgrader P, Ryvkin P, Bent ZW, Wilson R, et al. Massively parallel digital transcriptional profiling of single cells. Nat Commun 2017;8:14049.
- Hao Y, Hao S, Andersen-Nissen E, Mauck WM 3rd, Zheng S, Butler A, et al. Integrated analysis of multimodal single-cell data. Cell 2021;184: 3573–87.e29.
- 32. Becht E, McInnes L, Healy J, Dutertre CA, Kwok IWH, Ng LG, et al. Dimensionality reduction for visualizing single-cell data using UMAP. Nat Biotechnol 2019;37:38–44.